Accepted Manuscript

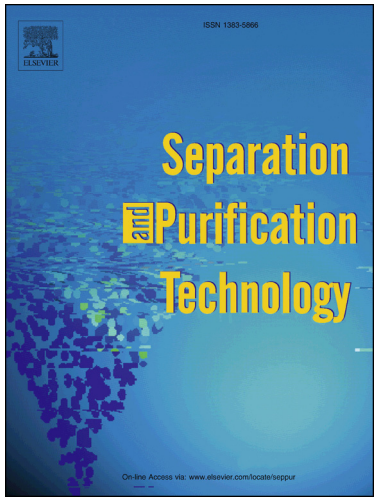

A review of the mechanisms and models of bubble-particle detachment in froth flotation

Guichao Wang, Anh V. Nguyen, Subhasish Mitra, J. B. Joshi, Graeme J. Jameson, Geoffrey M. Evans

PII: S1383-5866(16)30828-0
DOI: http://dx.doi.org/10.1016/j.seppur.2016.06.041
Reference: SEPPUR 13097

To appear in: *Separation and Purification Technology*

Received Date: 25 January 2016
Revised Date: 19 June 2016
Accepted Date: 24 June 2016

Please cite this article as: G. Wang, A.V. Nguyen, S. Mitra, J. B. Joshi, G.J. Jameson, G.M. Evans, A review of the mechanisms and models of bubble-particle detachment in froth flotation, *Separation and Purification Technology* (2016), doi: http://dx.doi.org/10.1016/j.seppur.2016.06.041

A review of the mechanisms and models of bubble-particle detachment in froth flotation

Guichao Wang[1*], Anh V. Nguyen[2], Subhasish Mitra[1], J. B. Joshi[3], Graeme J. Jameson[1], Geoffrey M. Evans[1]

[1]Discipline of Chemical Engineering, School of Engineering, University of Newcastle 2308, Australia

[2]School of Chemical Engineering, University of Queensland 4072, Australia

[3]Homi Bhabha National Institute, Mumbai 400094, India

* Author to whom all the correspondence should be addressed

Phone : +61 (2) 40339068, Fax: +61 (2) 40339095

Email: Guichao.wang@uon.edu.au

Abstract

Only when the process of particle detachment is well understood and modelled can minerals recovery using the flotation process be modulated to achieve a high efficiency by suitably changing the operating parameters. This is vitally necessary for the recovery of coarse particles in an energy efficient way, as detachment is the key limiting factor in the successful recovery of large particles. However, until the detachment mechanism is more fully understood, an upper limit on the floatable particle diameter still remains unidentified. To assess the current state of knowledge available in this area, a comprehensive literature review on the mechanisms and models of the bubble-particle detachment process in froth flotation is presented. In general, the detachment process is considered to be a stochastic process, and is usually attributed to the dynamic interactions with the turbulent flow structures (eddies) in the flotation environment which cause particles to detach because of dissipating energy. In this paper, previous studies on bubble-particle detachment have been critically analyzed with respect to the formulation of the models in predicting the detachment probability of particles. The models are classified into three different categories: force balance analysis; energy balance analysis and empirical analysis of particle size compared to maximum floatable particle size. Attention is also paid to an understanding of the mechanisms of bubble-particle detachment in quiescent and turbulent liquid flow fields. The predictions of all these models have been compared with the published experimental data and it was found that models which take an accurate consideration of the influence of eddies on a particle's detachment give the closest predictions. The generally held concept of bubble-particle detachment inside an eddy was experimentally validated, where a particle was observed to rotate on the surface of a bubble, resulting in a centrifugal acceleration 20 times that of gravitational acceleration. The aim of this paper is to review the developments and limitations of the existing models. The experimental work is reviewed so as to reveal the mechanisms of bubble-particle

detachment. Therefore, the future development of models is identified in order to successfully predict particle detachment.

Keywords: bubble-particle detachment; detachment model; turbulence; flotation

1. Introduction

Froth flotation is an important process in the mining industry, and is widely used in the recovery of valuable minerals from the ores. It is also applied in processes like the deinking of waste paper and in waste water treatment. The essence of flotation lies in using bubbles to capture particles based on their surface hydrophobicity difference. Hydrophobic particles are more likely to attach to the bubble interface due to a strong adhesion force compared to hydrophilic particles. The kinetics of flotation is often described as a first-order process, relating the rate of particle attachment to particle concentrations (Sutherland, 1948; Jowett and Safvi, 1960; Kelsall, 1961; Arbiter and Harris, 1962; Klassen and Mokrousov, 1963; Ahmed and Jameson, 1989). Following this definition, the rate of a particle capture process in a batch process can be described as:

$$\frac{dC_p}{dt} = -kC_p \tag{1}$$

where the rate constant, k, represents the rate of the removal of particles from the pulp, and C_p is the particle concentration in the pulp in units of mass/volume. It is noted that Equation (1) only applies to the simulated removal of particles in a batch process. In a continuous flotation cell, the inlet and outlet concentrations do not change with time in a steady state, so that Equation (1) does not apply to the cell as a whole. Batch flotation has been most extensively studied in the laboratory. The experimental data has been tested against a more general model:

$$\frac{dC_p}{dt} = -kC_p^n \tag{2}$$

where n is the order of the "reaction" between the particles and bubbles. Arbiter (1951) considered the second-order fit experimental data. Morris (1952) considered a first-order rate equation similar to Equation (1). When integrated, it gave:

$$k = \frac{1}{t} \ln \frac{C_0 - x}{C_t - x} \tag{3}$$

where C_0 is the original concentration of the mineral, C_t is the concentration after time t, and x is the percentage of unfloatable mineral.

Bushell (1962) used a modified first-order equation to fit his data, and gave:

$$\frac{dC_p}{dt} = -k(C_p - C_T) \tag{4}$$

Here, C_T is the concentration of unfloatable material. The fit of the function improved when C_T was taken as an empirical constant.

These expressions appear to be conflicting, and the reasons lie in the definitions of the rate constant k and the rate order n (Jameson et al. 1977). The critical parameter here is the rate constant k which, in fact, is not in any sense a constant. It is a proportionality factor that can be correlated to a particular set of conditions. The rate constant is typically expressed as a function of the physical parameters of the system (Arbiter, 1951; Morris, 1952; Jowett and Safvi, 1960; Bushell, 1962; Jameson, Nam et al., 1977; Gorain, Franzidis et al., 1995; Yoon and Mao, 1996; Gorain, Franzidis et al., 1997; Deglon, Sawyerr et al., 1999; Heiskanen, 2000) which can be written as:

$$k = \frac{3QhP_{collection}}{2d_b V_c}. \tag{5}$$

where Q is the gas volumetric flowrate, h is the depth of the cell, d_b is the bubble diameter, V_c is the effective volume of the cell, $P_{collection}$ is the probability that a particle can be collected in the pulp phase. The rate constant is dependent on the particle and bubble sizes,

and the way of dependency varies as the particle collection efficiency is strongly dependent on the particle's size. The particle collection process is decomposed into three incidences: the collision between the particles and bubbles; the particle attachment to the bubble; the particle detachment from the bubble. Thus, the probability that a particle that can be collected is:

$$P_{collection} = P_c P_a \left(1 - P_d\right) \tag{6}$$

where P_c is the collision probability, P_a is the attachment probability and P_d is the probability of a particle detachment from the bubble. It is apparent that the collision, attachment and detachment processes should be individually modelled so as to properly model the flotation process kinetics in order to successfully predict the product recovery rate from the limited known input variables. The recovery rate can be improved by manipulating these input variables. Flotation recovery typically depends on particle size. Initially, the flotation recovery increases with particle size monotonically and reaches a plateau. Afterwards, the flotation recovery plummets with an increase in particle size (Gaudin, 1931; Trahar, 1981; Dobby and Finch, 1987; Crawford and Ralston, 1988; De F. Gontijo et al., 2007). The reasons attributed to the decline in recovery rates for fine and coarse particles are reportedly different (Ralston et al., 1999; Jameson et al., 2007; Jameson, 2010). Due to their small inertias, the collision and attachment stages often become limiting factors for fine particle recovery. On the contrary, coarse particles, after forming bubble-particle aggregates, are vulnerable to disturbances from the adjacent liquid's motion, which results in particle detachment. Both the collision and attachment processes have been widely investigated and reported. Critical literature reviews on the collision models have been presented (Dai et al. 2000; Meyer and Deglon, 2011). On the attachment process, Nguyen et al. (1998) thoroughly studied the factors affecting this process. In a physical sense, particle attachment happens only when the induction time, defined as the time for the thin film between the particle and

the bubble to rupture, is longer than the contact time between a bubble-particle pair. Albijanic et al (2010) reviewed the roles of the induction and contact times in a study of the attachment process. It was noted that out of the three successive sub-processes of the bubble-particle interactions, the detachment process remains relatively unexplored for the reason that detachment is negligible for fine particles – the usual size range of interest in mineral processing industries. The modelling approaches in such cases assumes that, once attached, fine particles stay attached to the bubble, leading to complete recovery.

Nevertheless, the study of particle detachment from the bubble has its historical origins in the analyses of the forces on the particle attached to a fluid interface (Nutt, 1960; Princen, 1969). This theory was further developed by Schulze (1977; 1982). The mechanisms of particle detachment are complex because of the eddies and circulating flow patterns imposed on the pulp. From the perspective of the hydrodynamics, the various mechanisms of the detachment of particles from bubbles were discussed. Klassen and Mokrousov (1963) considered that the detachment of particles from bubbles was because of the destructive forces in a flotation process. The destructive forces may come from: (a) the rise (accelerated or equilibrium) of a mineralized bubble; (b) the actions of liquid streams; (c) the slide of a particle along a bubble; (d) a change in the motion of a bubble; (e) the impact and attrition of particles in the pulp against a mineralized bubble surface; (f) the impact of a bubble with an obstacle; and, (g) the oscillation of the bubble's surface. Woodburn et al. (1971) proposed that a particle could be wrenched from a bubble, to which it had adhered, by a sudden acceleration. Schulze (1982) hypothesized that a bubble-particle aggregate was entrapped into an eddy and that the attached particle followed the motion of the eddy in a centrifugal movement. When the centrifugal force is higher than the capillary force, the particle is detached.

It is worth noting that these analyses were based on bubble-particle interactions in the pulp phase and that the effect of the froth layer was not considered. The existence of a froth layer has a significant impact on particle detachment, especially at the pulp-froth interface (van Deventer et al., 2004). On the way up to the froth layer, the bubble-particle aggregates gradually decelerate due to a decrease in the medium's density which results in a subsequent reduction in the driving buoyancy force. It is believed that the abrupt change in velocity is sufficient to dislodge attached particles when the bubbles carrying the attached particles arrive at an air-water interface. The kinetic energy released by the deceleration and impact upon arrival at the interface causes the detachment of the particles (Falutsu, 1994). However, recent experiments by Ireland and Jameson (2014) have demonstrated, for the first time, that the particles do not detach as the arrival kinetic energy is dissipated by the motion of the particles. In the froth phase, the bubbles coated with particles tend to coalesce and result in a lower specific surface area. The combined effects of the increase in inertia, due to collision, and the decrease of the specific surface area lead to particle detachment. Particle detachment in the froth phase has attracted significant recent research attention (Ata et al., 2003; Ata, 2008; Ata, 2009; Ata, 2011; Ata, 2012; Ang et al., 2013). For the last few decades, the concept of coarse particle flotation has been gaining significant research attention in the mineral processing industries as significant amounts of energy can be saved in the grinding process (Austin, 1973; Jameson, 2010; Curry et al., 2014). It is known that, unlike for fine particles, the detachment sub-process is the limiting factor for the successful recovery of coarse particles in the flotation process. Due to such limitations, the option for extending the upper size limit of floatable particles is rather limited; however, this constraint can be relaxed by manipulating the hydrodynamic conditions of the flotation cell. The reasons behind the poor recovery rates of coarse particles was explored by Jameson (2012), based on experiments carried out by two separate research groups. Welsby et al. (2010) reported

careful on-site measurement of the rate constant for galena flotation, and the experimental data were analyzed with reference to particle size and surface liberation. Thereafter, Muganda et al. (2011) measured the effect of the contact angle on the flotation rate constants based on a size-by-size basis. It was observed that the particle size's influence on the flotation recovery followed a similar trend for particles of different levels of surface liberation. By combining these two interesting experimental results, Jameson (2012) explained that the poor recovery of coarse particles is independent of poor surface liberation, since even the fully liberated particles are affected in the same way with changes in the particles' sizes. This leads to an important conclusion that the hydrodynamic environment in flotation cells results in a decline in the recovery rates of coarse particles. More specifically, these hydrodynamic conditions are essentially governed by the fluctuating velocity components, i.e., the intensity of the turbulence in the pulp phase. It was shown that decreasing the level of intensity of the turbulence leads to the improved recovery of coarse particles of a given size (Jameson and Goel, 2012).

Although significant studies have reported on the bubble-particle detachment process, to the best of authors' knowledge there are no reviews which have reported on the bubble-particle detachment phenomenon to this date. This literature review is intended to summarize the previous bubble-particle detachment studies, with an emphasis on an in-depth analysis of the mechanisms and strengths and weaknesses of the various models reported. To avoid the complexities of inter-bubble-particle collision interactions in the froth phase, for which models are decidedly scarce, and which require further research, this review is constrained to a discussion only of the particle detachment process in the pulp phase.

2. Bubble-particle detachment models

2.1. Detachment models based on force balance

It is intuitive to study particle motions on a bubble's surface, either for an analysis of attachment or detachment, from the perspective of a force balance analysis following Newton's second law of motion. The forces acting on the particle can be divided into two groups: attaching forces and detaching forces. The competition between these two groups of forces governs the particle's detachment and stability. A particle will detach from a bubble interface if the magnitude of the detaching forces surpasses the magnitude of the attaching forces. To analyze the particle detachment process, the Bond number (*Bo*) is expressed as the ratio of the inertial force to the capillary force in order to characterize the stability of the bubble-particle aggregate. Following the above definition, in a general sense, the Bond number can be expressed as:

$$Bo = \frac{\rho g d^2}{\sigma} \tag{7}$$

where g is the gravity acceleration associated with the body force, ρ is the particle density, d is the characteristic length scale of a particle and σ is the surface tension of the interface. A high Bond number indicates that the system is relatively unaffected by the effects of surface tension, while a low Bond number indicates the dominance of a surface tension force.

Originally the importance of the Bond number was utilized in describing the two-phase system, for example the shape deformation of a droplet. Realizing the limitations of the Bond number in reflecting the actual physics of a three-phase flotation system, Schulze (1982) proposed a modified Bond number (B_o^*), which is expressed as the ratio of the magnitude of all off the detaching forces to all of the attaching forces. Thus, the modified Bond number is not restricted to a two-phase system, where only particles (droplets or bubbles) exist in a

continuum fluid, but is expanded to a multi-phase flotation system in describing a bubble-particle detachment where the particles, bubbles and liquid all coexist.

Logically, if particle detachment is considered to be a static process, where the detaching force is equal to, or exceeds, the attaching force, the particle should be detached. When a detaching force is less than an attaching force, particles stay attached to the bubble interface. The analysis of the bubble-particle detachment is under the assumption that there is a bubble-particle aggregate. The strength of a bubble-particle aggregate is the difference between the tenacity and the detaching forces. Figure 1 shows the strength of an aggregate changing with the particle's radius in a gravitational field. The defaulted applicability of a bubble-particle detachment is located in the domain (on the left side) of the bubble-particle aggregate. On the right-hand side, the detachment already occurs. Thus, the detachment probability is 1 when the detaching forces are higher than the tenacity of a bubble-particle aggregate. Consequently, a sharp separation can be expected in the flotation process, where particles bigger than a critical size will detach, and fine particles smaller than this critical size will stay attached to the bubble interface. Based on the definition of the modified Bond number (B_o^*), then the particle detachment probability can be defined as follows:

$$\begin{aligned} B_o^* \geq 1; P_d = 1 \\ B_o^* < 1; P_d = 0 \end{aligned} \tag{8}$$

From the definition of the modified Bond number, it can be readily realized that the particle detachment probability is proportional to the detachment force and is inversely proportional to the strength of the bubble-particle aggregate (Nguyen and Schulze, 2004). According to the experimental data (Plate et al., 1989) and the theoretical reasoning of the detachment probability presented in Equation (8), an exponential distribution function can be assumed to describe the particle detachment process. The detachment probability based on this concept is described as follows:

$$P_d = exp\left(-\frac{S}{F_{de}}\right) \tag{9}$$

where F_{de} is the detaching force and S is the strength of the bubble-particle aggregate, which is expressed as the difference between the tenacity and the detaching forces. Utilizing the definition of the modified Bond number, Equation (9) is further transformed and the probability of particle detachment (Schulze, 1993) can be expressed as follows:

$$P_d = exp\left(1-\frac{1}{B_o^*}\right) \tag{10}$$

Equation (10) presents the particle detachment probability model in its simplest form however it does not account for many factors, for example, the hydrodynamic conditions of the system. Often the mean liquid flow around the bubble-particle aggregate is taken into account to represent the hydrodynamic effect, in terms of the drag force on the bubble-particle aggregates. Although the effects of the hydrodynamic conditions due to the mean flow are relatively straightforward to include in the model, such is not the case with the fluctuating velocity components which generate turbulence of different length scales in the system. Bloom and Heindel (2002) studied the detachment frequency for flocs disruption in a turbulent field, and vortices with the size of a typical bubble-particle aggregate were thought to be responsible for the aggregate destruction. Analytical expressions for the bubble-particle detachment frequency were obtained.

The detachment probability model obtained in Equation (10) was modified by adding an additional stability constant A_s to match the experiment result:

$$P_d = exp\left[A_s\left(1-\frac{1}{B_o^*}\right)\right] \tag{11}$$

where A_s is an empirical constant that varies from 0 to 1.0. Assuming A_s is equal to 0.5, the variation of the particle detachment probability with B_o^* obtained from Bloom's model is

compared with Schulze's model in Figure 2. With the inclusion of this empirical constant, which captures the unaccounted system hydrodynamics, the detachment physics is apparently better represented, even though it is purely empirical and system specific with no other experimental validation available. It can be seen from Figure 2 that the predictions of the two probability distribution functions presented in Equation (10) and Equation (11) are different due to the change in slope. As the empirical constant A_s is restricted from 0 to 1.0 for the same B_o^*, Bloom's model predicts a higher detachment probability than Schulze's model. It should, however, be noticed that using these models, when B_o^* exceeds 1.0, a physically inconsistent detachment probability of higher than 1.0 is predicted. To avoid this limitation, the function prediction is restricted to 1.0 (the cut-off value) for any B_o^* value other than 1.0 for practical purposes. It is worth noting that at B_o^* = 1.0, when the sum of the attaching forces is equal to the sum of the detaching forces, a maximum floatable particle size can be obtained from the force balance analysis.

Bubble-particle aggregate stability depends, to a great extent, on the interplay of the different forces. Nutt (1960) studied the adhesion of a spherical particle to an air-liquid interface, where a centrifugal field was applied to detach the particle. For the given system's physical properties (contact angle, surface tension, liquid and solid density, etc.), the critical centrifugal force was theoretically calculated and was found to agree with the experimental results. A schematic of the particle detachment from the gas-liquid interface used in Nutt's study (1960) is presented in Figure 3. In this analysis, only three forces, namely the surface tension force, buoyancy force and centrifugal force, were considered. Of all these forces, the surface tension force (capillary force) is perhaps the most critical in a mineral flotation process (Yoon, 2000). The attachment of a particle to the bubble interface depends greatly on the capillary force which, in turn, depends on the radius of the three phase contact line, the

surface tension of the interface, and the contact angle (Amirfazli and Neumann, 2004; Chau et al., 2009).

In Figure 3, the bubble-particle aggregate is considered to be axisymmetric and the surface tension force in this system acts in the direction to the center of the bubble. It is apparent that such a definition of the surface tension force depends on the geometric location of the particle on the interface. In this case, the total surface tension force acting on the perimeter is calculated as follows:

$$F_c = 2\pi\sigma R_p \cos\alpha \cos(\pi - \theta - \alpha) \tag{12}$$

where R_p is the radius of the three phase contact angle, α is the polar angle of the interface position on the particle's surface (measured from the bubble rear) and θ is the contact angle obtained from drawing two tangents at the interface and at the intersection point of the interface and the particle surface.

The buoyancy force (F_b) is also a stabilizing force which can be evaluated from the mass of the liquid that would be contained in the cylinder (Figure 3), together with the spherical portion. It is:

$$F_b = \rho_l g \left\{ \begin{array}{l} \left(2\sigma / \rho_l g\right)^{1/2} \pi R_p^2 \cos^2\alpha \left[1 - \sin(\pi - \theta - \alpha)\right]^{1/2} \\ + \frac{4}{3}\pi R_p^3 - \frac{\pi}{3} R_p^3 (1 - \sin\alpha)^2 (2 + \sin\alpha) \end{array} \right\} \tag{13}$$

The centrifugal force acts on the bubble-particle aggregate to destabilize it. This force arises from the rotational motion of the surrounding liquid, and is expressed as:

$$F_a = \frac{4}{3}\pi {R_p}^3 \rho_p \, \mathrm{b}_m \tag{14}$$

where b_m represents the characteristic machine acceleration of the system. For a given system, there exists a value of angle α for which the sum of the surface tension force and the buoyancy force is the maximum. Therefore, the critical centrifugal acceleration (b_m) can be determined by counterbalancing the maximum attaching force.

Princen (1969) considered the influence of the particle's shape on the force balance on the particle at a fluid interface in quiescent conditions. Three shapes of particles, i.e., cylinder, prismatic particle and sphere were considered in analysis. The two forces considered were the surface tension force and a combined force of the apparent gravity and the hydrostatic pressure force. From the force balance of the considered forces, the critical radius of a particle was calculated. Particles larger than the critical size would just detach from the liquid interface. A complete force balance analysis of attached particles was further developed by Schulze (1977; 1982), who considering two distinct cases - a static case in a quiescent liquid and turbulent liquid motion incorporating the influence on the bubble-particle aggregates from eddies. From this study, the maximum size of a floatable particle of a given density was calculated as a function of the bubble size and the turbulence intensity or, in particular, the specific energy dissipation rate. This study was critical in forming the robust basis for determining the effects of the different forces on a bubble-particle's aggregate stability, and thus requires an elaborate analysis.

The static case in a quiescent liquid is described in Figure 4, where a spherical particle is attached to a bubble. It can be noticed that the central angle α, the angle between the vertical line and the radius to the point of the three phase contact, is different from the definition used in the analysis of Nutt (1960). The forces considered to act on the particle are, namely, the capillary force, buoyancy force, pressure force and the gravity force. In the forces analysis, positive and negative signs indicate the direction of the attaching force and the detaching force, respectively. The most significant attaching force is the capillary force. For a particle size of R_p, attached at the bubble-liquid interface, the capillary force can be expressed as:

$$F_c = 2\pi\sigma R_p \sin\alpha \sin(\theta - \alpha) \tag{15}$$

It is apparent that the capillary force is at its maximum when the polar angle α is half of the contact angle (Nguyen, 2003).

The second force which stabilizes the particle attached to a bubble is the buoyancy force. In a liquid of density ρ_l, for a partially immersed particle, the buoyancy force can be described as:

$$F_b = \frac{\pi R_p^3 \rho_l g}{3}\left(2 + 3\cos\alpha - \cos^3\alpha\right) \tag{16}$$

When it comes to the pressure force, there are two components acting in opposite directions. One component originates from the hydrostatic pressure, while the other one comes from the capillary pressure. Combining the contributions of these two components, the net pressure force is written as:

$$F_p = \pi R_p^2 \sin^2\alpha H \rho_l g - \pi R_p^2 \sin^2\alpha \frac{2\sigma}{R_b} \tag{17}$$

A positive sign for the hydrostatic pressure force makes it an attaching force, which is contributed to by the height of the liquid from the bubble's apex to the three phase contact area acting on the three phase contact area. It is represented by the first term of Equation (17). Due to the surface tension, the Laplace pressure inside the bubble is higher than the pressure outside the bubble. The capillary pressure force is determined by multiplying the pressure difference across the interface to the three phase contact area, and is represented by the second term of Equation (17).

The particle weight, F_g, which pulls the attached particle into the liquid, acts as a detaching force. For a particle with a density of ρ_p, the gravity force can be written as:

$$F_g = -\frac{4\pi R_p^3 \rho_p g}{3} \tag{18}$$

By considering the balance of all these forces acting on a bubble-particle aggregate at equilibrium, the maximum floatable particle size can be obtained. In contrast to the static case (stagnant fluid around the bubble-particle aggregate), where a consideration of the above discussed forces is sufficient to obtain an estimate of the maximum floatable particle size,

such is not the case with an actual flotation cell where a turbulent flow condition persists. In his analysis, Gaudin (1957) showed that the maximum floatable size of minerals, from such a force balance consideration, can be larger than the maximum particle size of an actual flotation process by a factor of 10. Such an anomaly exists because, in a flotation cell, the bubble-particle aggregates are subjected to other disruptive forces due to the turbulent fluid's motion which are not accounted for by the force balance model in the static case. To describe such detaching/disruptive forces, Schulze (1982) considered the interaction of the rotating turbulent flow structures (eddies) with the bubble-particle aggregate and postulated that the centrifugal force originating from the rotating flow structures detaches the particle from the bubble when the bubble-particle aggregate is trapped in a rotating eddy. This theory is based on the assumption that a bubble-particle aggregate trapped in an eddy of the same scale will rotate along the eddy to the extent where the centrifugal force exceeds the adhesive force.

Particles with a density higher than the continuous phase tend to migrate from the center of eddies to the ridge of the flow structure. On the contrary, the bubbles, due to their smaller density, tend to gather in the center of flow structures. Such distribution patterns of particles and bubbles determine the stability of the bubble-particle aggregates in the turbulent field. The particles present in the turbulent eddy are moved by the corresponding size of the turbulent eddies. It is apparent that obtaining an expression of the centrifugal force, while considering the complex heterogeneous nature of the turbulence, is not a trivial matter. However, a simpler expression for the centrifugal force can be obtained, assuming isotropic turbulence, following Kolmogorov's theory:

$$F_a = -\frac{4\pi R_p^3 \rho_p b_m}{3} \tag{19}$$

where b_m is the turbulent acceleration generated by the eddies, and which can be determined by the root mean square of the fluctuating velocities $\overline{u_l}$ over the rotating length scale r, as follows:

$$b_m = \frac{\overline{u_l}^2}{r} \tag{20}$$

To determine the fluctuating velocity, the energy levels of the eddies is considered to be in the inertial sub-range (Kolmogorov, 1941):

$$\overline{u_l} = c_1 (\varepsilon l)^{1/3} \tag{21}$$

where c_1 is a constant equal to 1.37, l is the distance of the particle rotation from the reference axis located inside the eddy and ε is the specific kinetic energy dissipation rate. Schulze (1982) assumed that the particles move with the same velocity as the eddy, and the radius of rotation can be represented by the bubble diameter, d_B. Substituting u_l from Equation (21) into Equation (20), then, the centrifugal accelerationb_m, can be rearranged as:

$$b_m = 1.9\varepsilon^{2/3} / d_B^{1/3} \tag{22}$$

The description of the fluctuating velocity component in Equation (21) was further modified by Hui (2001). In his work, the value of c_1 was reduced to 1.5 and the radius of rotation was replaced with the radius of the bubble-particle aggregate instead of the previously used bubble diameter. Using these new values, the maximum acceleration of the aggregate can be found out as:

$$b_m = 2.38\varepsilon^{2/3} / d_{ag}^{1/3} \tag{23}$$

When the bubble-particle aggregate is in the vicinity of an eddy with a diameter of the same order of magnitude to its size, it is hypothesized that the interactions between the aggregate and the eddy will result in bubble vibration, leading to the rotational motion of the attached particle on the bubble surface. Two distinct accelerations are considered to act on the attached particle in this case, namely circulation and vibration acceleration. The rotational velocity of the attached particle on the vibrating bubble surface can be approximated as follows:

$$u_{ps} = 2\pi r_s \left(u'\kappa\right) \tag{24}$$

where r_s is the radius of the particle movement on the bubble surface, u' is the liquid fluctuating velocity, κ represents eddies of κ -space. Following this, the circulation acceleration can be expressed as follows:

$$b_{cir} = 4\pi^2 r_s \left(u'\kappa\right)^2 \tag{25}$$

.

For a favorable interaction between the bubble-particle aggregate and the eddies following the transfer of energy, the individual eddy size should be in the same order of magnitude as the aggregate. With the size of the eddy equal to the diameter of the bubble-particle aggregate, one can obtain the following expression for the circulation acceleration:

$$b_{cir} = 2\pi^2 c_1 \frac{\varepsilon^{2/3}}{d_{ag}^{1/3}} \tag{26}$$

To describe the vibration acceleration of the aggregate, an analogy with a spring-mass system could be drawn. Upon external excitation, for example, with energy transfer due to interaction with the eddies, the bubble vibrates like a spring. The maximum vibration acceleration of the attached particle can be expressed by:

$$b_v = \left(2\pi u'/ d_{ag}\right)^2 A \tag{27}$$

where A is the amplitude of the bubble vibration, which is proportional to the bubble diameter. Assuming the amplitude follows a linear trend with the bubble radius as $c_2 \frac{d_{ag}}{2}$, the vibrational acceleration can be expressed as follows:

$$b_v = 2\pi^2 c_1 c_2 \frac{\varepsilon^{2/3}}{d_{ag}^{1/3}} \tag{28}$$

Combining these two accelerations together, the effective acceleration can be expressed as:

$$b_{\max} = 2\pi^2 c_1 \left(1 + c_2\right) \frac{\varepsilon^{2/3}}{d_{ag}^{1/3}} \tag{29}$$

From the definition of the bubble vibration amplitude, it is reasonable to assume that c_2<<1. Thus, the acceleration of the attached particle maybe expressed as:

$$b_m = 29.6\varepsilon^{2/3} / d_{ag}^{1/3} \tag{30}$$

Hui (2001) assumed the detachment probability as:

$$P_d = exp\left(-\frac{F_{at}}{F_{de}}\right) = exp\left(-\frac{2\sigma(1-\cos\theta)}{d_P^2\Delta\rho\left(g+29.6\varepsilon^{2/3}/d_{ag}^{1/3}\right)}\right) \tag{31}$$

Usually, in the flotation situation the eddy turbulent acceleration is typically more than 100 times the gravitational acceleration. Considering the aggregate diameter as the bubble diameter, Equation (31) becomes:

$$P_d = exp\left(-\frac{\sigma(1-\cos\theta)d_B^{1/3}}{14.8d_P^2\Delta\rho\varepsilon^{2/3}}\right) \tag{32}$$

In another work, Koh and Schwarz (2005) used a similar equation with a different length scale in reference to Schulze (1982), where the particle size is taken into considerations. It is:

$$b_m = 1.9\varepsilon^{2/3} / \left(d_B + d_P\right)^{1/3} \tag{33}$$

Goel and Jameson (2012) assumed that the radius of the rotation is equal to the radius of the bubble. So, the attached particle is considered to rotate at the same speed as the interacting eddy of the same size as the bubble. The equation for the eddy turbulent acceleration is given as follows:

$$b_m = 3.75\varepsilon^{2/3} / d_B^{1/3} \tag{34}$$

There are a number of similarities in the definitions of eddy turbulent acceleration. The capture of bubble-particle aggregates by the rotating eddies is, rather, a hypothesis of the particle detachment process which has not been experimentally validated. Actually, the interactions of particles with eddies is of practical importance in many technological and environmental applications. The dispersion patterns of the particles resulted from their

interactions with eddies are different, depending on the particle's density relative to the continuous phase (Crowe et al., 1995).

By analyzing the forces at work on the attached particle, and comparing the attaching force to the detaching force, bubble-particle detachment can be predicted. Based on Schulze's definition of the modified Bond number, which is a ratio of the detaching force on the attaching force, it is:

$$B_o^* = \frac{F_g - F_b + F_a + F_p}{F_c} \tag{35}$$

Note that the capillary force depends on the position of the three phase contact line on the particle, and that in the modified Bond number expression the capillary force is replaced with a maximum capillary force when the central angle α is half of the contact angle. The maximum floatable particle size is present when B_o^* is 1, which means that the particle is detached when B_o^* is larger than 1. A simple calculation can show why large particles are vulnerable to detachment caused by turbulent flow. The force of detachment is proportional to the particle's mass, which is linear with the cubic of the particle size. The adhesive force changes with the perimeter length of the three phase contact line, between the particle, the liquid and the air bubble, which is proportional to the particle's size. Thus, B_o^*, which is a ratio of the detachment force to the adhesion force, is approximately proportional to the square of the particle's size. Correspondingly, there is a maximum particle size of a given density to a certain turbulent intensity. Schulze (1993) defined this dimensionless number in order to characterize aggregate stability, in which the capillary force was the maximum. This can be achieved at a specific situation when the central angle is half of the contact angle.

Replacing the forces, the modified Bond number is written as:

$$B_o^* = \frac{d_P^2\left(g\Delta\rho + \rho_P b_m\right) - d_P\sigma\cos^2\left(\frac{\theta}{2}\right)}{6\sigma\sin^2\left(\frac{\theta}{2}\right)} \tag{36}$$

Thus, Schulze (1993) gave the detachment probability as:

$$P_d = \exp\left\{1 - \frac{6\sigma\sin^2\left(\frac{\theta}{2}\right)}{d_P^2\left(g\Delta\rho + \rho_P b_m\right) - d_P\sigma\cos^2\left(\frac{\theta}{2}\right)}\right\} \tag{37}$$

Goel and Jameson (2012) made a simplification by just considering the capillary force and the centrifugal force and gave a formula on the modified Bond number in relation to the turbulent energy dissipation rate. Substituting the eddy centrifugal acceleration, the modified Bond number is:

$$B_o^* = 3.75\frac{d_P^2\rho_P\varepsilon^{2/3}/d_B^{1/3}}{6\sigma\sin^2\left(\frac{\theta}{2}\right)} \tag{38}$$

and the detachment probability is:

$$P_d = \exp\left(1 - \frac{6\sigma\sin^2\left(\frac{\theta}{2}\right)}{3.75 d_P^2\rho_P\varepsilon^{2/3}/d_B^{1/3}}\right) \tag{39}$$

It is noted that the modified Bond number has been used to study bubble-particle detachment. The significance of the modified Bond number equation is that it can predict the maximum floatable size of a particle of a given density and contact angle in a flotation cell with a known energy dissipation rate (Jameson and Goel, 2012).

Nguyen and Schulze (2004) studied particle detachment caused by different mechanisms and external forces, including gravitational forces, tensile stresses, shear stress and bubble vibrations. A number of equations can be derived from the different perspectives. The

detachment probability is written as an exponential function of the attaching force and the detaching force:

$$P_d = exp\left(1-\frac{F_{att}}{F_{de}}\right) \tag{40}$$

In a flow field dominated by tensile stress, the detaching force is a combination of the gravity force and the centrifugal force. Then, the detachment probability is:

$$P_d = exp\left(1-\frac{3\sigma\left(1-\cos\theta\right)}{4R_P^2\left(g+b_m\right)\Delta\rho}\right) \tag{41}$$

It is worth noting that the theory on formulating capillary force presented in the literature so far has not considered the dynamic contact angle. Due to the movement of the gas-liquid interface over a solid surface, the three phase contact line has a certain velocity which is responsible for the contact angle hysteresis and leads to a transient change in the contact angle (Ngan and Dussan, 1982; Drelich et al., 1996; Kwok and Neumann, 1999; Gao and McCarthy, 2006; Kowalczuk and Drzymala, 2011). The contact angle, therefore, in reality changes from the assumed static contact angle over the course of the dynamics of the detachment process. In contrast to the measurement of the static contact angle, which is usually measured in a straightforward way by the sessile droplet/bubble method, the measurement of the dynamic contact angle is rather challenging since no single value can be reported due to the changing nature of the contact angle over time. Usually, a limit is rather imposed on the range of the dynamic contact angle, in terms of the advancing (maximum) and receding (minimum) contact angle, which are usually measured by the increasing or decreasing liquid volume of the sessile or pendent droplet. Another method is to impart rotational motion to a sessile droplet resting on a sample stage to the point of the incipient motion of the droplet. Such controlled experiments are not able to include the surrounding environmental effects on the transient nature of the dynamic contact angle, for example, the

influences of the surrounding fluid's movement, which is the case for real applications like the flotation process where the bubble-particle aggregate is subject to the turbulent liquid's motion around it. This physical quantity, although difficult to measure, is extremely significant in formulating the capillary force, which is the prime attaching force for the particle on a bubble's surface. Due to the inability of measuring the dynamic nature of the contact angle, as well as the absence of a robust physical model, often the capillary force is modelled by incorporating the equilibrium contact angle or the static contact angle, which is independent of the movement of the three phase contact line. Theoretically, the equilibrium contact angle can be derived from Young's hypothesis that the interfacial forces achieve an equilibrium state at the three phase contact point. The equilibrium contact angle derived in this way assumes any value between the advancing contact angle and the receding contact angle. Looking closely at the bubble-particle interaction, it is apparent that particle detachment from a bubble's surface is a wetting process, during which the three phase contact does not move while the contact angle is changing until the advancing contact angle is reached. In contrast, particle attachment is rather a dewetting process, during which the three phase contact perimeter only expands when the apparent contact angle is less than the receding contact angle. The difference between the advancing contact angle and the receding contact angle is described as contact angle hysteresis which can be expressed as:

$$\Delta\theta = \theta_A - \theta_R \ . \tag{42}$$

The magnitude of the capillary force is dependent on the length of the three phase contact line, which in turn depends on the particle position (polar angle) on the attached bubble's surface. The maximum magnitude of the force is obtained when the polar angle subtended at the center of the particle (α_m) becomes half of the contact angle. In the particle attachment process this central angle is higher than the receding contact angle, since $\alpha_R = \theta + \beta$, as per the schematic presented in Figure 5. Depending on the position of the particle on the bubble's

surface, the local interface shape deformation pattern may vary around the three phase contact line (see Figure 4 and Figure 5). Figure 4 shows a particle attached to the bottom of a bubble with the interface stretched away from the center of the bubble, which reflects the onset of a necking phenomenon typical of the particle detachment process due to the downward direction of the gravity force. The depth of a particle's penetration into the bubble depends on the attaching process. The contact angle reaches the minimum contact angle at the receding contact angle. At the end stage of particle attachment, the three phase contact line stops expanding and the central angle reaches the maximum at α_R. When α_R is higher than α_m, where the maximum capillary value is achieved, in the process of detachment the central angle α keeps on reducing and the capillary force keeps on increasing until the central angle reaches α_m. Otherwise, if α_R is smaller than α_m, the capillary force does not have the opportunity to reach its theoretical maximum value and the capillary force is highest when the central angle is at its maximum, that is α_R. Thus, Nguyen and Schulze (2004) concluded that Equation (41) is valid when α_m is smaller than α_R. When α_m is higher than α_R, the particle is detached after the contact angle exceeds the advancing contact angle. This condition $\Delta\theta \geq \theta_R$ applies while taking the smallest value of the central angle at α_R. The capillary force is changed, and replacing it into Equation (41) gives:

$$P_d = exp\left(1 - \frac{3\sigma \sin\theta_R \sin(\Delta\theta)}{4R_P^2 (g + b_m)\Delta\rho}\right), \Delta\theta \geq \theta_R \tag{43a}$$

when $\Delta\theta \leq \theta_R$, replacing the equilibrium contact angle in Equation (41) with the advancing contact angle, the detachment probability is:

$$P_d = exp\left(1 - \frac{3\sigma(1 - \cos\theta_A)}{4R_P^2 (g + b_m)\Delta\rho}\right), \Delta\theta \leq \theta_R \tag{43b}$$

In the same way, in a flow field dominated by shear stress detachment, the probability is an exponential function of the attaching force and the detaching force. The difference is to analyze the competence between the shear force and the capillary force component in the tangential direction. The bubble-particle couplet was experimentally observed to be sheared apart (Wang et al., 2016). Similarly, the detachment probability is:

$$P_d = exp\left(1-\frac{\sigma\left(1-\cos\theta_A\right)\sin\left(\Delta\theta/2\right)}{0.26\pi R_P\rho_l\sqrt{\varepsilon\nu}}\right), \Delta\theta \le \theta_R \tag{44a}$$

$$P_d = exp\left(1-\frac{\sigma\sin\theta_R\sin(\Delta\theta)\sin\left(\Delta\theta/2\right)}{0.13\pi R_P\rho_l\sqrt{\varepsilon\nu}}\right), \Delta\theta \ge \theta_R \tag{44b}$$

Tao (2005) described detachment probability as

$$P_d = \frac{1}{1+F_{att}/F_{de}} \tag{45}$$

where F_{att} is the total attachment force and F_{de} is the total detachment force. This suggests that when the detachment force is equal to the attachment force, $P_d = 0.5$; $P_d = 0$ when $F_{att} >> F_{de}$; $P_d = 1$ when $F_{att} << F_{de}$. The detachment probability is:

$$P_d = \frac{1}{1+\dfrac{3\sigma\left(1-\cos\theta_d\right)}{g\left\{\rho_P-\rho_l\pi\left[1/2+3/4\times\cos\left(\theta_d/2\right)\right]\right\}}\dfrac{1+d_P/d_B}{d_P^2}} \tag{46}$$

2.2. Detachment models based on energy balance

Yoon and Mao (1996) gave the probability of detachment from the perspective of energy, where the detachment probability was considered to be an exponential function of the energy ratio. The energy considered is the energy supplied to the attached particle and the energy required for the detachment to occur. In the process of detachment, two kinds of energy need to be overcome, i.e., the work of adhesion and the energy barrier. A particle can be detached

when the kinetic energy that tears the particle off the bubble's surface exceeds the energy (work of adhesion, W_a, and energy barrier, E_1). The detachment probability is written as:

$$P_d = exp\left(-\frac{W_a + E_1}{E_k^{'}}\right) \tag{47}$$

where W_a is the work of adhesion calculated as follows:

$$W_a = \sigma\pi R_p^2 \left(1-\cos\theta\right)^2 \tag{48}$$

and E_1 is the energy barrier. Yoon and Mao (1996) used kinetic energy to predict detachment by considering a simple situation, where a cap of particles attaches to the bottom of a rising bubble, as is shown in Figure 6. As bubbles rise in a flotation cell, more and more particles will be collected at the bottom of the bubble. The kinetic energy is supplied by the fluid flowing past the bubble and the particle at the center is subjected to a pressure p_1. The particles in the cap are subjected to increased pressure. The kinetic energy of the particle is calculated as follows:

$$E_k^{'} = p_1\phi \tag{49}$$

where ϕ is the area of contact between the particle and the bubble. It is given by:

$$\phi = \pi R_p^2 sin^2\theta \tag{50}$$

The particle in the center of the cap is subjected to a pressure p_1:

$$p_1 = \frac{\rho_P g R_B^2 \theta_0}{3} \tag{51}$$

where ρ_P is the particle density, g is the gravitational acceleration, R_B is the bubble radius and θ_0 is the cap angle reflecting the loading capacity of the bubble, which is a function of the number of the particles in the cap. When θ_0 is zero, there is no particle on the bubble. As the bubble rises up, the number of particles collected on the bubble's surface increases. So

does the energy exerted on the attached particle. Inserting Equation (50) and Equation (51) into Equation (49) gives the following prediction for the kinetic energy for detachment:

$$E_k^{'} = \frac{\rho_P g R_B^2 \theta_0}{3} \pi R_P^2 \sin^2\theta \tag{52}$$

Hence, the probability of detachment is:

$$P_d = exp\left(-\frac{\sigma\pi R_p^2 \left(1-\cos\theta\right)^2 + E_1}{\frac{\rho g R_B^2 \theta_0}{3} \pi R_P^2 \sin^2\theta} \right) \tag{53}$$

The limitation of this model is that it is derived for a quiescent environment. Sherrell (2004) extended this model to describe particle detachment in a turbulent field generated by an impeller. The largest eddy within the flotation cell is created by the impeller itself. It is assumed that the energy contained in the largest eddy directly corresponds to the bubble-particle aggregate detachment. The kinetic energy is equal to the tip-velocity of the impeller squared:

$$U_D^2 = \left(R_{imp}\omega\right)^2 \tag{54}$$

then, the turbulent energy provided to the bubble-particle aggregate is:

$$E_k^{'} = \frac{1}{2}\left(m_p + m_b\right) U_D^2 \tag{55}$$

Usually, the energy barrier is negligible compared to the work of adhesion. Thus, the detachment probability can be written as:

$$P_d = \exp\left(-\frac{\sigma\pi R_p^2 \left(1-\cos\theta\right)^2}{\frac{1}{2}\left(m_p + m_b\right)\left(R_{imp}\omega\right)^2} \right) \tag{56}$$

As noted, Equation (56) is fitted for a turbulent flow field generated by an impeller. Do (2010) gave a general model for turbulent flow where the velocity was calculated from the shear rate. Referring to Camp and Stein (1943), the shear rate inside an eddy is $\sqrt{\varepsilon/\nu}$. For a bubble-

particle aggregate inside an eddy, the velocity of the attached particle, in respect to the bubble, is $(d_P + d_B)\sqrt{\varepsilon/\nu}$. The kinetic energy of the particle is described by:

$$E_k^{'} = \frac{1}{2} m_p \left((d_P + d_B)\sqrt{\varepsilon/\nu} \right)^2 \tag{57}$$

The detachment probability is given as:

$$P_d = \exp\left(-\frac{\sigma\pi R_p^2 (1-\cos\theta)^2}{\frac{1}{2} m_p \left((d_P + d_B)\sqrt{\varepsilon/\nu} \right)^2} \right) \tag{58}$$

Nguyen and Schulze (2004) also gave the detachment probability from an energy perspective, which is given as:

$$P_d = exp\left(1 - \frac{\Delta E_{de}}{E_k^{'}} \right) \tag{59}$$

ΔE_{de} is the particle energy of the detachment, which is calculated as follows:

$$\Delta E_{de} = \sigma\pi R_p^2 (1-\cos\theta)^2 \times C \tag{60}$$

where C is the correction to the thermodynamic estimation of the particle detachment energy. It is:

$$C = \frac{1}{4} \ln \frac{2L/R_P / \sin(\theta/2)}{e^{\gamma} \cos^2(\theta/4)} + \frac{13 + 16\cos(\theta/2) + 7\cos\theta}{64\cos^4(\theta/4)} \tag{61}$$

where L is the capillary length, γ is the Euler constant and is equal to 0.5772, θ is the contact angle and R_p is the particle radius. $E_k^{'}$ is the detaching energy due to the turbulent fluctuations:

$$E_k^{'} = \frac{4\pi R_p^3 \Delta\rho}{3} \frac{(\Delta V)^2}{2} \tag{62}$$

where $\Delta\rho$ is the density difference between the attached particle and the liquid, ΔV is the turbulent relative velocity of the bubble-particle aggregate. Thus, the detachment probability is described as follows:

$$P_d = exp\left(1-\frac{3\sigma\left(1-\cos\theta\right)^2\times C}{2R_P\Delta\rho\left(\Delta V\right)^2}\right) \tag{63}$$

Wang et al. (2014) developed a bubble-particle detachment model from an energy perspective. With the accurate account of kinetic energy supplied from the turbulent liquid's motion, eddies of the same scale in the close vicinity of the attached particles are considered accountable for the particle's detachment. In this way, the detachment probability is written as:

$$P_d = \exp\left(-\frac{8\sigma R_p^2\left(1-\cos\theta\right)^2}{c\rho_l\varepsilon^{2/3}d_p^{11/3}}\right) \tag{64}$$

2.3. Detachment models based on maximum floatable particle size

Many other researchers have studied the probability of particle detachment from an empirical perspective. The detachment probability is correlated with the particle size in reference to the maximum floatable particle size. Woodburn et al. (1971) developed a model capable of predicting recovery for any particular particle size range, giving the following equation to represent the particle detachment probability in reference to the maximum floatable size, d_{pmax}:

$$P_d = \begin{cases} \left(\frac{d_p}{d_{pmax}}\right)^{1.5}, \mathrm{d_p} \le \mathrm{d_{pmax}} \\ 1, \mathrm{d_p} > \mathrm{d_{pmax}} \end{cases} \tag{65}$$

Jameson et al. (2007) provided the following equation:

$$P_d = exp\left(1-\left(\frac{d_{p\max}}{d_p}\right)^2\right) \tag{66}$$

The maximum particle size that could remain attached to a bubble was given by Nguyen (2003), where the equation derived by Schubert (1999) was combined with the work of Schulze (1982). It is:

$$d_{p\max} = \left(\frac{3\sigma\left(1-\cos\theta\right)}{\Delta\rho\left(g+b_m\right)}\right) \tag{67}$$

In deciding the centrifugal acceleration, the maximum stable bubble size from Parthasarathy et al. (1991) was used:

$$d_{b\max} = 3.27\left(\frac{\sigma^{3/5}}{\varepsilon^{2/5}\rho_l^{3/5}}\right) \tag{68}$$

Inserting the maximum stable bubble size into Equation (22) gives:

$$b_m = 1.28\varepsilon^{4/5}\rho_l^{1/5}/\sigma^{1/5} \tag{69}$$

Thus, the detachment probability can be expressed as:

$$P_d = exp\left(1-\frac{2.34\sigma^{6/5}\left(1-\cos\theta\right)}{d_p^2\Delta\rho\varepsilon^{4/5}\rho_l^{1/5}}\right), \Delta\theta \le \theta_R \tag{70a}$$

This equation is valid when the contact angle hysteresis is less than the receding contact angle. When the contact angle hysteresis is larger than the receding contact angle, Equation (70a) is replaced by:

$$P_d = exp\left(1-\frac{1.17\sigma^{6/5}\sin\theta_R\sin\Delta\theta}{d_p^2\Delta\rho\varepsilon^{4/5}\rho_l^{1/5}}\right), \Delta\theta \ge \theta_R \tag{70b}$$

Brożek and Młynarczykowska (2010) proposed the following formula:

$$P_d = \left(\frac{d_p - d_{p\min}}{d_{p\max} - d_{p\min}}\right)^n \tag{71}$$

where d_{pmin} is the size of the floating particle, below which the detachment probability is zero, d_{pmax} is the size of the particle above which the detachment probability is 1, and n is an empirical constant.

3. Experimental works

Although force balance models were proposed to analyze the bubble-particle aggregate's stability, the direct measurement of these forces was not performed up until Butt's (1994) work which is reportedly considered to be pioneering work in measuring the force between a particle and a bubble in water using an atomic surface microscope (AFM). In the AFM measurement technique, the deflection of the cantilever during the process of pulling out a glass particle from a bubble was measured to translate into the interaction forces. Further work was carried out by Pitois (2002) who studied the effects of the contact angle hysteresis on the force and work of detachment using an AFM. The effects of the contact line pining and the associated contact angle hysteresis on the force and the work to detach a particle was quantified in his work. The measurement of the force-path curve showed that neglecting the contact angle hysteresis during the detachment process could induce significant deviations. Further work on the contact angles was carried out by Nguyen (2003), where an AFM was used to determine the contact angle for fine particles, and it was observed that the contact angle of a spherical particle changed with the speed of the AFM piezoelectric translator. The dynamic behavior of the contact angle and other uncertainties, such as the position of the three phase contact line on the particle's surface during the bubble-particle interaction, make it difficult to directly use the experimentally determined contact angle as a measure of the particle surface hydrophobicity. Schimann (2004) measured the detachment force between spherical particles of varying hydrophobicity and air bubbles using a surface tensiometer. In

his work, bubble-particle detachment was defined as a three step process. The first step involves bubble stretching caused by surface tension and the contact angle hysteresis. Once the advancing contact angle is reached, the three phase contact line begins to slide off the particle, which is defined as step two. The final step of particle detachment is the formation of a bubble neck which narrows down with time till a breakup point is reached. Afterwards, the adhered particle detaches from the bubble and leaves a small amount of air attached to the particle. An illustration of how the colloid probe technique can be used to measure single bubble-particle interactions and the contact angle can be found in the literature review (Johnson et al. 2006). Ally (2010) measured the detachment force needed to detach a micro-particle from an air-liquid interface with different solutions in order to study the effects of surface tension and viscosity. The results showed that the maximum force during detachment was not necessarily at the position where the particle broke away from the interface. This can be explained by the dynamics of meniscus deformation and the viscosity effects. Taran and Nguyen (2012) offered a better qualification of the local bubble deformation by modelling AFM measurements by solving the augmented Young Laplace equation with the inclusion of DLVO disjoining pressure. Bubble deformation revealed the nonlinear behavior of the local bubble-liquid interface deformation. This outcome can help to convert the actual AFM data into force versus separation distance. In summary, advanced experimental methods make detachment force measurement available. It is beneficial to understanding the mechanism of the bubble-particle detachment process. Even though the detachment force can be accurately measured, the shortcoming of this technique is its inability to reflect the conditions (the liquid's motion) under which particle detachment occurs.

Researchers have devised different experimental techniques to study particle detachment in different conditions. Nutt (1960) devised an experimental technique using a centrifuge method to detach the particle from a liquid's interface. Schulze (1989) used a similar method

to determine the adhesive strength of particles within the liquid/gas interface, where single particles were attached to the liquid's surface. The liquid was placed in a glass cell of a laboratory centrifuge with a freely swinging rotor. By increasing the speed to a given value, particles were exposed to increasing centrifugal accelerations. The decisive advantage of this method is its applicability in studying the essential characteristics of a single micro-process of flotation, namely the stability of bubble-particle aggregates, by changing the rotation speed to get rid of other influencing parameters.

Holtham and Cheng (1991; 1995) studied the particle detachment process in flotation using an acoustic vibration method. A small loudspeaker driven by an audio signal generator was used to provide sinusoidal vibration to a small rectangular glass cell where a single bubble with a known number of attached particles was settled. The experimental detachment force was compared with the theoretically predicted attachment forces, and the results showed that the amplitude of the oscillations imposed on the bubble was the dominant factor in the detachment process. This can be reflected in the significant deformation of air bubbles in coarse particle flotation due to collision with large particles. The oscillating bubble causes a prevalence of particle detachment. Stevenson et al (2009) studied the behavior of an oscillating particle attached to a gas liquid surface, and three more forces, i.e., Basset history force, the added mass of the particles and the drag force imparted by the liquid, were added to analyze the true position of the three phase contact line. The results showed that the Basset history force, drag force, d'Alembert force and capillary force were dominant over the particle weight, buoyancy and pressure force due to meniscus deformation.

To fully and explicitly explain the function of the energy dissipation rate on the flotation process, Brady et al. (2006) simulated a flotation column environment by passing pulp through a grid of cylindrical rods. The fluctuating velocities of the particle and bubble were calculated and compared to theoretical models based on the turbulent energy dissipation rate.

Grid oscillation was believed to generate nearly isotropic and homogeneous turbulence (Long, 1978; De Silva and Fernando, 1994; Srdic et al., 1996; Shy et al., 1997; Kang and Meneveau, 2008), which is beneficial to study the turbulence's influence on the flotation kinetics. Further, the oscillating grid flotation cell was devised to exhibit relatively isotropic and homogeneous turbulence, characterizing the effects of energy input on the flotation kinetics (Changunda et al., 2008; Massey et al., 2012). The results showed that the power intensity influence on the flotation kinetics was strongly dependent on both the particle and bubble size. Increasing the energy input for fine particle flotation benefits the flotation recovery. An optimum energy input is beneficial for coarse particle flotation because a higher energy input leads to particle detachment. Omelka et al. (2009; 2010) studied the detachment of particles from bubbles in the wake turbulence behind grids. The particle detachment was due to the breakage of bubbles in the strong shear flow, and particle detachment due to centrifugal force was not observed.

To float coarse particles, a special flotation process is needed. Jameson (2008; 2010) devised a new process for coarse particle flotation in which a fluidized bed was formed in the flotation cell to bring the particle and bubble into contact in a quiescent environment. The flow conditions in this flotation cell are very gentle and high solid concentration ensures a rapid rate of particle capture, which leads to a high flotation recovery rate.

Xu et al. (2011) examined the detachment of coarse particles from oscillating bubbles as a function of the particle's hydrophobicity and shape, as well as a medium's viscosity. The schematic diagram of the apparatus is shown in Figure 7. The results showed that the quasi-static model predicts the detachment force quite well at low vibration frequencies. At high vibration frequencies the model cannot make an accurate prediction because of the reason that the detachment force is determined by the dynamic contact angle, which is governed by the velocity of the three phase contact line. The rate of movement of the three phase contact

line is reduced at high viscosity, resulting in more stable bubble-particle aggregates. Awatey et al. (2014) used this technique to measure the detachment forces for particles with different contact angles. The detachment forces of the particles increased with the contact angle, indicating a lower detachment probability for particles with a higher contact angle. The critical detachment amplitude was also plotted as a function of the measured contact angle, showing a higher critical detachment amplitude is needed to detach particles with higher contact angles. This technique was later used by Fosu et al. (2015) to test the detachment of coarse composite particles from bubbles. Particles with the same contact angle but different sizes responded to vibration differently, in that coarser particles detach at lower acceleration due to high inertia. However, as noted in the experiment on the movement of the bubble, the frequency and magnitude of the movement of the bubble was assumed to be identical with that of the loudspeaker. This is true without considering the elasticity of the bubble. Nevertheless, for the bubble size (typically 2 mm in diameter) used in the experiment, neglecting the bubble deformation in the process of oscillation is evidently inappropriate.

The testing of particle detachment as a function of the energy dissipation rate in a turbulent liquid field is only recently available (Goel and Jameson 2012). As shown in Figure 8, a specially designed flotation cell was devised to observe the behavior of particle-laden bubbles in a turbulent shear flow, where Schulze's hypothesis and the criterion for detachment are tested. Bubbles were generated in a fluidized bed, where particles adhered to the bubble. The bubbles were then directed beneath the impeller into the cell, and some particles were observed to detach. The fractional detachment of particles was related to the mechanical energy dissipation rate in the region of the impeller, and the results showed that detachment occurred over a range of modified Bond numbers. It does not support the hypothesis that detachment occurs at the critical Bond number of 1. Nevertheless, Schulze's detachment criterion was within the correct order of magnitude. However, as the energy dissipation rate

in a stirred tank is distributed unevenly, even at the impeller region, how particles get detached with the impaction from the surrounding vortices is still not clear.

Wang et al. (2016) designed a novel experimental setup to study bubble-particle detachment in a turbulent vortex. As is shown in Figure 9, a vortical flow field develops in the wall cavity when water flows through the tunnel. A bubble that was pre-loaded with one or more particles was introduced into the cavity, and the motion of the bubble-particle aggregate was studied using a high-speed video camera. The trajectories of the attached particles in a centrifugal motion on the bubble's surface were analyzed in order to prove the validity of the theory that the centrifugal force leads to particle detachment. Figure 10 shows a time series of the centrifugal movement of a spherical particle on a bubble's surface. The particle diameter was 282 μm and the bubble diameter was 715 μm, and the particle was seen to rotate about the bubble at 143 cycles per second, giving a centrifugal acceleration of 297 m/s^2. The rotational speed of an attached particle can reach as high as 200 cycles per second and the averaged centrifugal acceleration leading to detachment of particles was nearly 23 times the gravitational acceleration. For the first time, the centrifugal movement of a particle on the bubble's surface inside a vortex was observed, and the theory of detachment due to centrifugal movement in the turbulent field was experimentally proven.

It is noted that the direct measurement of the detachment force of a particle detaching from a bubble using AFM provides insights into the bubble-particle detachment process. The only problem with this method is that the detachment force is measured statically by gradually increasing the load on the cantilever. It is an efficient way to measure bubble-particle aggregate strength, but is far from reflecting particle detachment in a real flotation situation. Particle detachment is reflected in the study of the effect of particle size on the flotation process as a whole, where recovery drops for coarse particle flotation (Awatey et al., 2013, Jameson, 2012, Trahar, 1981, Woodburn et al., 1971, Morris, 1952, Gaudin et al., 1931).

Considering the complexity of bubble-particle detachment in a real flotation environment, methods like the centrifugal method and the oscillation method are devised to mimic the particle's behavior, such as its rotation and oscillation. The detachment probability can be reflected by the amplitude of oscillation or the rotation speed. Keeping in track with the detachment models, the influence of the liquid's motion is reflected in the detachment probability prediction by the energy dissipation rate. An oscillating grid device is used to study the influence of energy input on the flotation recovery. The limitation is that the flotation is considered as a whole process. Furthermore, a delicate experiment, where the bubble-particle aggregates are introduced into a stirred tank, is used to study the energy dissipation rate's influence on bubble-particle detachment. For the first time, the detachment probability was plotted as a function of the energy dissipation rate and experimentally testified as a function of the modified Bond number. The mechanisms of bubble-particle detachment remained unclear until recent experimental work on bubble-particle detachment in a rotating eddy. The detachment of particles due to centrifugal movement was proven for the first time and centrifugal acceleration can reach 20 times the gravitational acceleration.

4. Summary of discussions

In previous sections, the different detachment models have been reviewed and grouped into three principal categories, namely, force, energy and maximum floatable particle size. Intuitively, a particle's movement on a bubble's surface, whether detaching or staying attached, depends on the forces acting on the bubble. The bubble-particle detachment process was analyzed from the perspective of the force balance. Table 1 presents the various detachment models reported in the literature obtained from the force balance analysis. Of all the forces, in a typical flotation environment, the centrifugal force is believed to be

responsible for bubble-particle detachment in turbulent flow fields (Abrahamson, 1975; Schulze, 1977). The centrifugal force is dependent on the interactions between the eddies and the bubble-particle aggregate. Solid particles with a density higher than the fluid phase tend to migrate away from the eddy's core and concentrate on the edges of the eddy. Bubbles with a density smaller than the liquid phase tend to gather in the eddy's core. Conspicuously, a bubble-particle aggregate interacts with an eddy differently than the usual interaction behavior of its counterparts – the individual bubble and particle.

The discrepancies between the models in calculating the centrifugal force comes from the eddy's turbulent acceleration, where the radius of the rotation is rooted in the definition of the aggregate's movement inside an eddy. Schulze (1982) considered that the radius of the rotation is equal to the bubble's diameter, while Hui (2001) regarded the diameter of the bubble-particle aggregate as the rotation radius. Goel and Jameson (2012) considered that the bubble-particle aggregate was captured in the center of the eddy and that the radius of rotation was the bubble's radius. Theoretically, when the attached particles are negligible to the bubble or if the bubble is fully covered by tiny particles, where the bubble is considered to be a heavier bubble but much lighter than the fluid phase, the aggregate will act more like a bubble. When the aggregate interacts with an eddy, it will migrate to the center of the eddy. In contrast, an aggregate will rotate with the eddy diverted from the center when the attached particle becomes more dominant over the bubble. Schubert (1978; 1999) studied the hydrodynamics inside flotation machines, and various eddy sizes were observed. Three sub-processes of flotation controlled by the turbulence were discussed. Even though the way in which bubble-particle aggregates interact with eddies has not been proven, it can be concluded that the bubble-particle detachment happens due to the centrifugal field of the turbulent eddies (Zhang et al., 2016).

In the particle detaching process, the capillary force is the attaching force that stops a particle from detaching and the capillary force changes with the contact angle. Nguyen and Schulze (2004) pointed out that the contact angle hysteresis was required to be taken into consideration when calculating the maximum capillary force. When the contact angle hysteresis is less than the receding contact angle, the capillary force is at a maximum with the polar angle at half of the advancing contact angle. When the contact angle hysteresis is higher than the receding contact angle, the capillary force is at a maximum with the polar angle at the highest value equal to the receding contact angle. In different conditions, the respective maximum capillary force expression is replaced in the detachment probability prediction. A bubble-particle aggregate interacting with an eddy will not only experience centrifugal force, but also shear stress. Under shear stress, the three phase contact meniscus is no more symmetrical. The net component of the capillary force in the tangential direction comes into being to counterbalance the shear force. This net component of the capillary force depends on the contact angle hysteresis. When the shear force is higher than the net component of the capillary force, the particle is detached. Thus, Nguyen and Schulze (2004) gave the particle detachment probability by comparing the shear force and the capillary force component in the tangential direction.

Detachment probability is predicted as an exponential function of the forces. When the detaching force is equal to the attaching force, the detachment probability is 1. Tao (2005) gave the detachment probability as inverse to the force ratio. When the detaching force equals the attaching force, whether the particle is attaching or detaching, it counts as 0.5 percent individually. Also, only when the attaching force is negligent to the detaching force, the detachment probability is infinitely close to 1. Contrariwise, when the attaching force is much larger than the detaching, the force detachment probability is close to 0. Thus, for a given system, the detachment probability is always within a certain range between 0 and 1.

The detachment probability is also predicted from the perspective of the energy balance, as is shown in Table 2. When the energy required to detach the attached particle is met, the particle is going to detach. Yoon and Mao (1996) assumed that the detachment probability is an exponential function of the energy ratio and gave the expression for a bubble rising up in a stationary liquid. The detachment energy is provided by the pressure acting on the particle seated at the bottom of the bubble. The default limitation of this model is that it is suited to stationary liquid and the detaching energy is provided by other particles seated above the particle at the bottom. Considering that just one particle is attached to the bubble, it will not detach, no matter the size of the particle. Sherrell (2004) extended this expression to describe the particle detachment in a stirred tank. The detachment energy is considered to be provided by the largest eddy in the tank, which is generated by the stirrer. Do (2010) generalized particle detachment in a turbulent field by considering the shear rate acting on the bubble-particle aggregate. The relative velocity between the particle and the bubble is considered as the provider of the detachment energy. The relative velocity is calculated by multiplying the shear rate by the bubble-particle aggregate's size. Wang (2014) took into consideration the influence of the turbulent liquid's motion in the way that the energy required to detach the particle was provided by the kinetic energy of the liquid's motion. In a turbulent liquid field, the bubble carrying the attached particles would experience a range of eddies of different scales. The bubbles would follow the large scale liquid's motion, which is in a bigger scale than the bubble's size. For eddies of the same scale or smaller than the bubble's size act on the bubble's surface and affect the particle's performance on the bubble's surface. Eddies of the same scale as the attached particles transfer kinetic energy to the attached particles. The similarity between these models is that even where enough energy is provided for the particle to detach, the detachment probability is 36.8 percent. Only where the detachment energy is much higher than the energy required, the detachment probability is close to 1. Similarly,

Nguyen and Schulze (2004) provided the detachment probability from an energy perspective by applying the same format as the force balance analysis. When the detachment energy is equal to the energy required for the particle to detach, the detachment probability is 1.

The detachment probability is also given for particles of different sizes compared to the maximum floatable particle size, as is shown in Table 3. Even though it is totally empirical, it can predict the detachment probability for particles of any given size for a flotation cell. Woodburn et al. (1971) used 1.5 orders of the diameter ratio (particle size on maximum floatable particle size) to calculate the detachment probability. When the particle's size is bigger than the maximum floatable particle size, the detachment probability is defaulted to 1. Jameson et al. (2007) used an exponential function to calculate the detachment probability. When the particle size is equal to the maximum floatable particle size, the detachment probability is 1. However, when the particle size is bigger than the maximum floatable particle size, the detachment probability is higher than 1. As the probability is within 0 to 1, so when the particle size is larger than the maximum particle size the detachment probability is defaulted to 1. Brożek and Młynarczykowska (2010) showed the detachment probability as a function of the partition number. This equation is applied to particle sizes in the range of the maximum floatable particle size and particle sizes below which no detachment occurs. Based on the empirical dependences obtained in a particular flotation machine, this stochastic model can predict the detachment probability from the particle's size.

From the above analysis, some models are for the static case and some models include the influences from the turbulent liquid's motion. Even though the turbulence's influence is interpreted from different perspectives, resulting in particle rotation or oscillation, the hydrodynamics inside the flotation cells are regarded as the main reason for the particle's detachment. It is difficult to solely study the influence of turbulence on the detachment of particles from bubbles, as the flotation process is usually studied as a whole. Omelka et al.

(2009; 2010) studied particle detachment in the wake turbulence behind grids, and the particle detachment was observed to occur due to the breakage of the bubble. It is noted, however, that the size of the bubbles used in the experiment were in the range of 1.7-4.5 mm, and the turbulence intensity was high, with the energy dissipation rate in the range of 50-100 m^2/s^3. In a turbulent flow with so high an energy dissipation rate, the bubbles are unstable and break into smaller bubbles, leaving particles detached. Connecting the probability of particle detachment in a turbulent liquid field as a function of energy dissipation rate is only recently available (Goel and Jameson, 2012). The experimental procedure was well designed so that only the detachment process was subjected to the turbulence's influence. As shown in Figure 8, a capillary system buried in a column of a fluidized bed was used to generate single bubbles. The particle-laden bubbles were directed beneath the impeller into a stirred tank. Particle detachment was observed in the turbulent shear flow. The fractional detachment of particles was related to the kinetic energy dissipation rate in the region of the impeller. In this part, the detachment probabilities calculated from the different models are compared with the experimental results.

The parameters used in the calculation are consistent with the experimental values, where the particle's diameter is 260 microns; the bubble's diameter is 1.5 mm; the contact angle is 50 degrees; the surface tension is 0.068 N/m; the liquid density is 1000 kg/m^3; the particle density is 2500 kg/m^3; and the impeller diameter is 50 mm. The rotation speed of the stirrer was modulated to provide different levels of turbulence and the detachment fraction was measured. Correspondingly, the detachment probability is calculated as a function of the energy dissipation rate.

Figure 11 compares the detachment probability from the force balance. It is apparent that Hui's model predicts a higher detachment probability, even at a low energy dissipation rate. It fast reaches close to 1 and stays almost constant at 1. As the detachment probability is

considered to be an exponential function of the force ratio of the attaching force on the detaching force, even the detaching force is much higher than the attaching force and the detachment probability is close to 1. Comparatively, Goel's model and Schulze's model predict a lower increasing slope as the particle detachment is due to centrifugal motion. Hui's model considers that turbulence leads to bubble oscillation and provides a much higher detaching force. Additionally, detachment probability is also calculated from the maximum floatable particle size using Jameson's model. In the range of the energy dissipation rate, Schulze's model is fit for a low energy dissipation rate and Jameson's model is fit for an energy dissipation rate of medium value. However, Hui's model predicts the detachment probability well when the energy dissipation rate is low, due to the characteristics of the assumed distribution function. Deviations may also come from the calculation of the energy dissipation rate. In the stirred tank, Goel and Jameson assumed that the detachment of particles occurs only in the vicinity of the impeller region, where most of the energy is dissipated. The mean energy dissipation rate is calculated for the region of the stirrer. More importantly, the local energy dissipation rate is more significant to bubble-particle detachment, other than the mean energy dissipation rate. Generally, the hypothesis of the centrifugal force in the eddy field predicts the detachment probability well at low levels of turbulence. Nevertheless, in a high level of turbulence this theory tends to exaggerate the influence from the turbulent liquid's motion.

The detachment probability is also calculated from energy perspectives. Figure 12 shows that the detachment probability increases sharply with the energy dissipation rate at a low turbulence level, which is far away from the experimental results. This is mainly due to the reason that the detachment is correlated with the energy required to supply a surface energy increment and the energy supplied to the particle from turbulent liquid's motion. Two factors lead to the overestimation of the energy's influence on particle detachment. One side is that

only the surface energy increment of the bubble replaces the three phase contact plane. However, in the detachment process a bubble is adsorbing and dissipating energy, to a large extent, due to its elastic property. Even though this amount is not clear in the detachment process, it is believed to be much higher than the surface energy increment. The other side is the way in which the energy is transferred from the liquid's motion to the attached particle. The particle is believed to follow the liquid's motion and the velocity is calculated from the levels of the turbulence's intensity using the energy dissipation rate. This neglects the particle's inertia and gravity, which overestimate the energy imparted on the attached particle from the turbulent liquid's motion. These two combined effects overestimate the influence of the turbulent liquid, making the detachment probability sensitive to an energy dissipation rate increase when the value is very small. Due to the assumed exponential function, the detachment probability remains constant at a high energy dissipation rate. The detachment probability prediction of Wang is also plotted. With a more accurate account of an eddy's influence, the model predicts the particle detachment in accordance with the experimental results, giving a closer prediction of the detachment probability over other models.

Bubble-particle detachment is a complex process. Under different flow conditions, the main characteristic features of the bubble-particle detachment differ. It can be summarized that all of the existing models somehow consist of empirical descriptions of the bubble-particle detachment. The detachment models of force balance and energy supply treat the influence of a turbulent liquid's motion differently, using either centrifugal force or kinetic energy. Nevertheless, the turbulence's influence on particle detachment is explained as the interaction of the eddy with the bubble-particle aggregate. The bubble-particle aggregate experiences different eddies on its way up to the froth phase. This stochastic process is described using a presumed distribution function, which is an exponential function. The distribution of the detachment probability still remains mysterious. Schulze and Stöckelhuber

(2005) cited Bloom and Heindel (2003) as a reference for Equation (11), where As was introduced. In turn, Bloom and Heindel got their equation from Schulze (1993). However, neither of them take us back to the original thesis of Plate, which is unpublished.

The success of the flotation process intuitively depends on controlling the bubble-particle aggregate's stability, which ensures the maximum recovery of floatable particles. Such control is only possible if the interactions of the aggregates with the surrounding turbulent fluid's motion are adequately understood. In recent years, researchers have started to use computational fluid dynamics (CFD) to simulate the behavior inside flotation cells (Koh et al., 2000; Koh and Schwarz, 2003; Koh and Schwarz, 2005; Koh and Schwarz, 2007; Kostoglou et al., 2007; Koh and Schwarz, 2008; Koh and Schwarz, 2008; Koh et al. 2009; Liu and Schwarz, 2009; Liu and Schwarz, 2009; Koh and Schwarz, 2011; Koh and Smith, 2011). The advantage of this approach is the potential to model any tank design at any scale, providing a wealth of details, such as the internal velocities, shear rates, turbulence parameters, distributions of phases, bubble sizes, and residence time distribution (Evans et al., 2008). Thus, the levels of turbulence inside flotation devices can be optimized to achieve high flotation recovery rates. The detailed understanding of flow gained using this approach allows modifications to existing equipment and the identification of potential process improvements (Koh and Schwarz, 2011). To achieve that, the flotation process needs to be well modelled.

5. Conclusion

This work has reviewed the different models for predicting bubble-particle detachment probability and the experimental work on bubble-particle detachment. The experimental work is focused on exploring the mechanisms of particle detachment. Using AFM can accurately

measure the detachment force. The particle detachment process is characterized by three processes: bubble stretching; three phase contact contraction and neck formation. However, it cannot represent particle detachment in a real flotation situation. The different methods are devised to study particle detachment under different conditions, like the centrifugal method, the oscillation method, an oscillating grid cell and a stirred tank. Thus, the influences on particle detachment of the speed of rotation, the magnitude of oscillation, the frequency of oscillation and the energy dissipation rate can be quantified. Nevertheless, bubble-particle detachment in a turbulent liquid's motion is not clearly understood. When a novel experiment was designed to capture the bubble-particle detachment process in a rotating eddy using high speed camera, the particles were observed to rotate on the surface of bubbles and the centrifugal acceleration reached 20 times the gravitational acceleration.

In the modelling of the particle detachment process a great disagreement exists in describing the influences of eddies and the interactions of eddies and bubble-particle aggregates. The models employed in describing detachment probability are divided into three groups: force balance, energy balance and maximum floatable particle size. As particle detachment is a stochastic process, certain distribution functions are assumed when describing the detachment probability, like the exponential distribution. The differences and similarities of the different models were analyzed. It is important to point out that the predictions of detachment probability from a particle's size based on the maximum floatable particle size are empirical, but are useful for the known flotation cells. In summary, the different detachment models were summarized and compared in this comprehensive literature review. The mechanisms of particle detachment are also discussed. Decreasing the energy input is considered as an efficient way to increase the flotation recovery of coarse particles. Hopefully, this organization of the knowledge on bubble-particle detachment will help researchers in floating coarse particles. Thus, future work in this area should aim to combine

the study of turbulence with bubble-particle detachment prediction. Once achieved, bubble-particle detachment can be predicted in a more direct way using the fundamental analysis of the inside physics, with less dependency on case specific empirical factors.

References:

Abrahamson, J., 1975. Collision rates of small particles in a vigorously turbulent fluid. Chem. Eng. Sci., 30(11): 1371-1379.

Ahmed, N., Jameson, G.J., 1989. Flotation kinetics. Miner. Process. Extr. Metall. Rev., 5(1-4): 77-99.

Albijanic, B., Ozdemir, O., Nguyen, A.V., Bradshaw, D., 2010. A review of induction and attachment times of wetting thin films between air bubbles and particles and its relevance in the separation of particles by flotation. Adv. Colloid Interface Sci., 159(1): 1-21.

Ally, J., Kappl, M., Butt, H.-J.r., Amirfazli, A., 2010. Detachment force of particles from air−liquid interfaces of films and bubbles. Langmuir, 26(23): 18135-18143.

Amirfazli, A., Neumann, A.W., 2004. Status of the three-phase line tension: a review. Adv. Colloid Interface Sci., 110(3): 121-141.

Ang, Z.J., Bournival, G., Ata, S., 2013. Influence of frothers on the detachment of galena particles from bubbles. Int. J. Miner. Process., 121: 59-64.

Arbiter, N. (1951). Flotation rates and flotation efficiency, Trans. AIME, 791: 796.

Arbiter, N., Harris, C.C., 1962. Flotation kinetics in froth flotation. 50th Anniversary vol. AIMME: 215-246.

Ata, S., 2008. Coalescence of bubbles covered by particles. Langmuir, 24(12): 6085-6091.

Ata, S., 2009. The detachment of particles from coalescing bubble pairs. J. Colloid Interface Sci., 338(2): 558-565.

Ata, S., 2011. The role of frother on the detachment of particles from bubbles. Miner. Eng., 24(5): 476-478.

Ata, S., 2012. Phenomena in the froth phase of flotation - A review. Int. J. Miner. Process., 102-103: 1-12.

Ata, S., Ahmed, N., Jameson, G., 2003. A study of bubble coalescence in flotation froths. Int. J. Miner. Process., 72(1-4): 255-266.

Austin, L.G., 1973. A commentary on the Kick, Bond and Rittinger laws of grinding. Powder Technol., 7(6): 315-317.

Awatey, B., Skinner, W., Zanin, M., 2013. Effect of particle size distribution on recovery of coarse chalcopyrite and galena in Denver flotation cell. Can. Metall. Q., 52(4): 465-472.

Awatey, B., Thanasekaran, H., Kohmuench, J.N., Skinner, W., Zanin, M., 2014. Critical contact angle for coarse sphalerite flotation in a fluidised-bed separator vs. a mechanically agitated cell. Miner. Eng., 60: 51-59.

Bloom, F., Heindel, T.J., 2002. On the structure of collision and detachment frequencies in flotation models. Chem. Eng. Sci., 57(13): 2467-2473.

Bloom, F., Heindel, T.J., 2003. Modeling flotation separation in a semi-batch process. Chem. Eng. Sci., 58(2): 353-365.

Brady, M.R., Telionis, D.P., Vlachos, P.P., Yoon, R.-H., 2006. Evaluation of multiphase flotation models in grid turbulence via Particle Image Velocimetry. Int. J. Miner. Process., 80(2–4): 133-143.

Brożek, M., Młynarczykowska, A., 2010. Probability of detachment of particle determined according to the stochastic model of flotation kinetics. Fizykochemiczne Problemy Mineralurgii, 44: 23-34.

Bushell, C., 1962. Kinetics of flotation.. Trans. AIME 223: 266-278.

Butt, H.-J., 1994. A Technique for Measuring the Force between a Colloidal Particle in Water and a Bubble. J. Colloid Interface Sci., 166(1): 109-117.

Camp, T.R., Stein, P.C., 1943. Velocity gradients in internal work in fluid motion. Cambridge, J. Boston Soc. Civ. Eng., 30, 219.

Changunda, K., Harris, M., Deglon, D.A., 2008. Investigating the effect of energy input on flotation kinetics in an oscillating grid flotation cell. Miner. Eng., 21(12-14): 924-929.

Chau, T.T., Bruckard, W.J., Koh, P.T.L., Nguyen, A.V., 2009. A review of factors that affect contact angle and implications for flotation practice. Adv. Colloid Interface Sci., 150(2): 106-115.

Cheng, T.-W., Holtham, P.N., 1995. The particle detachment process in flotation. Miner. Eng., 8(8): 883-891.

Crawford, R., Ralston, J., 1988. The influence of particle size and contact angle in mineral flotation. Int. J. Miner. Process., 23(1–2): 1-24.

Crowe, C.T., Troutt, T.R., Chung, J.N., 1995. Particle Interactions with Vortices. In: Green, S. (Ed.), Fluid Vortices. Fluid Mechanics and Its Applications. Springer Netherlands.

Curry, J.A., Ismay, M.J.L., Jameson, G.J., 2014. Mine operating costs and the potential impacts of energy and grinding. Miner. Eng., 56: 70-80.

Dai, Z., Fornasiero, D., Ralston, J., 2000. Particle–bubble collision models — a review. Adv. Colloid Interface Sci., 85(2–3): 231-256.

De F. Gontijo, C., Fornasiero, D., Ralston, J., 2007. The Limits of Fine and Coarse Particle Flotation. Can J Chem Eng, 85(5): 739-747.

De Silva, I.P.D., Fernando, H.J.S., 1994. Oscillating grids as a source of nearly isotropic turbulence. Phys Fluids, 6(7): 2455-2464.

Deglon, D.A., Sawyerr, F., O'Connor, C.T., 1999. A model to relate the flotation rate constant and the bubble surface area flux in mechanical flotation cells. Miner. Eng., 12(6): 599-608.

Do, H., 2010. Development of a Turbulent Flotation Model from First Principles, Ph.D. thesis, Virginia Polytechnic Institute and State University.

Dobby, G.S., Finch, J.A., 1987. Particle size dependence in flotation derived from a fundamental model of the capture process. Int. J. Miner. Process., 21(3–4): 241-260.

Drelich, J., Miller, J.D., Good, R.J., 1996. The Effect of Drop (Bubble) Size on Advancing and Receding Contact Angles for Heterogeneous and Rough Solid Surfaces as Observed with Sessile-Drop and Captive-Bubble Techniques. J. Colloid Interface Sci., 179(1): 37-50.

Evans, G.M., Doroodchi, E., Lane, G.L., Koh, P.T.L., Schwarz, M.P., 2008. Mixing and gas dispersion in mineral flotation cells. Chem. Eng. Res. Des., 86(12): 1350-1362.

Fosu, S., Skinner, W., Zanin, M., 2015. Detachment of coarse composite sphalerite particles from bubbles in flotation: Influence of xanthate collector type and concentration. Miner. Eng., 71(0): 73-84.

Gao, L., McCarthy, T.J., 2006. Contact Angle Hysteresis Explained. Langmuir, 22(14): 6234-6237.

Gaudin. A.M, Henderson. H.B, 1931. Effect of particle size in flotation. American Institute of Mining Engineers Technical Publication (414): 3-23.

Gaudin, A.M., 1957. Flotation. McGraw-Hill, New York, USA.

Goel, S., Jameson, G.J., 2012. Detachment of particles from bubbles in an agitated vessel. Miner. Eng., 36–38(0): 324-330.

Gorain, B.K., Franzidis, J.P., Manlapig, E.V., 1995. Studies on impeller type, impeller speed and air flow rate in an industrial scale flotation cell — Part 1: Effect on bubble size distribution. Miner. Eng., 8(6): 615-635.

Gorain, B.K., Franzidis, J.P., Manlapig, E.V., 1997. Studies on impeller type, impeller speed and air flow rate in an industrial scale flotation cell. Part 4: Effect of bubble surface area flux on flotation performance. Miner. Eng., 10(4): 367-379.

Heiskanen, K., 2000. On the relationship between flotation rate and bubble surface area flux. Miner. Eng., 13(2): 141-149.

Holtham, P.N. and Cheng, T.-W. Study of probability of detachment of particles from bubbles in flotation. Transactions of the Institution of Mining and Metallurgy, Section C: Mineral Processing and Extractive Metallurgy, 1991. (100): 147-153

Hui, s., 2001. Three-phase mixing and flotation in mechanical cells. Ph.D. thesis, University of Newcastle.

Ireland, P.M., Jameson, G.J., 2014. Collision of a rising bubble–particle aggregate with a gas–liquid interface. Int. J. Miner. Process., 130(0): 1-7.

Jameson, G., Nam, S., Young, M. M., 1977. Physical factors affecting recovery rates in flotation. Miner. Sci. Eng., 9(3), 103-118.

Jameson, G., Nguyen, A., Ata, S., 2007. The flotation of fine and coarse particles. Froth Flotation: A Century of Innovation. SME, Denver, CO, USA, 329-351.

Jameson, G.J., 2008. Method and Apparatus for Flotation in a Fluidized Bed. PCT Patent Application No. WO 2008/104022.

Jameson, G.J., 2010a. Advances in fine and coarse particle flotation. Can. Metall. Q., 49(4): 328-330.

Jameson, G.J., 2010b. New directions in flotation machine design. Miner. Eng., 23(11-13): 835-841.

Jameson, G.J., 2012. The effect of surface liberation and particle size on flotation rate constants. Miner. Eng., 36–38(0): 132-137.

Jameson, G.J., Goel, S., 2012. New approaches to particle attachment and detachment in flotation, Separation Technologies for Minerals, Coal and Earth Resources, Denver, Colorado. 437-445.

Johnson, D.J., Miles, N.J., Hilal, N., 2006. Quantification of particle-bubble interactions using atomic force microscopy: A review. Adv. Colloid Interface Sci., 127(2): 67-81.

Jowett, A., Safvi, S., 1960. Refinements in methods of determining flotation rates. Transactions of the American institute of mining and metallurgical engineers, 217, 351-357.

Kang, H.S., Meneveau, C., 2008. Experimental study of an active grid-generated shearless mixing layer and comparisons with large-eddy simulation. Phys Fluids, 20(12).

Kelsall, D.F., 1961. Application of probability in assessment of flotation systems. Institution of Mining and Metallurgy General Meeting: 191-204.

Klassen, V.I., Mokrousov, V.A., 1963. An introduction to the theory of flotation. Butterworths, London, UK.

Koh, P., Schwarz, P., 2011. A novel approach to flotation cell design. SME Annual Meeting and Exhibit, Denver, CO, 315-319.

Koh, P.T.L., Hao, F.P., Smith, L.K., Chau, T.T., Bruckard, W.J., 2009. The effect of particle shape and hydrophobicity in flotation. Int. J. Miner. Process., 93(2): 128-134.

Koh, P.T.L., Manickam, M., Schwarz, M.P., 2000. CFD simulation of bubble-particle collisions in mineral flotation cells. Miner. Eng., 13(14-15): 1455-1463.

Koh, P.T.L., Schwarz, M.P., 2003. CFD modelling of bubble-particle collision rates and efficiencies in a flotation cell. Miner. Eng., 16(11): 1055-1059.

Koh, P.T.L., Schwarz, M.P., 2005. CFD modelling of bubble-particle attachments in a flotation cell. Centenary of Flotation Symposium, Brisbane, QLD, 201-207.

Koh, P.T.L., Schwarz, M.P., 2007. CFD model of a self-aerating flotation cell. Int. J. Miner. Process., 85(1-3): 16-24.

Koh, P.T.L., Schwarz, M.P., 2008a. Computational fluid dynamics modelling of slimes flotation at Mt Keith operations. MetPlant 2008 - Metallurgical Plant Design and Operating Strategies, Perth, WA, 325-337.

Koh, P.T.L., Schwarz, M.P., 2008b. Modelling attachment rates of multi-sized bubbles with particles in a flotation cell. Miner. Eng., 21(12-14): 989-993.

Koh, P.T.L., Smith, L.K., 2011. The effect of stirring speed and induction time on flotation. Miner. Eng., 24(5): 442-448.

Kolmogorov, A.N., 1941. The local structure of turbulence in incompressible viscous fluid for very large Reynolds number. Dokl. Akad. Nauk SSSR, 30: 301-305.

Kostoglou, M., Karapantsios, T.D., Matis, K.A., 2007. CFD Model for the design of large scale flotation tanks for water and wastewater treatment. Industrial & Engineering Chemistry Research, 46(20): 6590-6599.

Kowalczuk, P.B., Drzymala, J., 2011. Contact Angle of Bubble with an Immersed-in-Water Particle of Different Materials. Ind. Eng. Chem. Res, 50(7): 4207-4211.

Kwok, D.Y., Neumann, A.W., 1999. Contact angle measurement and contact angle interpretation. Adv. Colloid Interface Sci., 81(3): 167-249.

Liu, T.Y., Schwarz, M.P., 2009a. CFD-based modelling of bubble-particle collision efficiency with mobile bubble surface in a turbulent environment. Int. J. Miner. Process., 90(1–4): 45-55.

Liu, T.Y., Schwarz, M.P., 2009b. CFD-based multiscale modelling of bubble–particle collision efficiency in a turbulent flotation cell. Chem. Eng. Sci., 64(24): 5287-5301.

Long, R.R., 1978. Theory of turbulence in a homogeneous fluid induced by an oscillating grid. Phys Fluids, 21(10): 1887-1888.

Massey, W.T., Harris, M.C., Deglon, D.A., 2012. The effect of energy input on the flotation of quartz in an oscillating grid flotation cell. Miner. Eng., 36-38: 145-151.

Meyer, C. J., Deglon, D. A., 2011. Particle collision modeling - A review. Miner. Eng., 24(8), 719-730.

Morris, T., 1952. Measurement and evaluation of the rate of flotation as a function of particle size. Mining Engineering, 4(8), 794-798.

Muganda, S., Zanin, M., Grano, S.R., 2011. Benchmarking flotation performance: Single minerals. Int. J. Miner. Process., 98(3-4): 182-194.

Ngan, C.G., Dussan V., E.B., 1982. On the nature of the dynamic contact angle: an experimental study. J. Fluid Mech., 118: 27-40.

Nguyen, A.V., 2003. New method and equations for determining attachment tenacity and particle size limit in flotation. Int. J. Miner. Process., 68(1–4): 167-182.

Nguyen, A.V., Nalaskowski, J., Miller, J.D., 2003. The dynamic nature of contact angles as measured by atomic force microscopy. J. Colloid Interface Sci., 262(1): 303-306.

Nguyen, A.V., Ralston, J., Schulze, H.J., 1998. On modelling of bubble–particle attachment probability in flotation. Int. J. Miner. Process., 53(4): 225-249.

Nguyen, A.V., Schulze, H.J., 2004. colloidal science of flotation. Marcel Dekker, New York, USA.

Nutt, C.W., 1960. Froth flotation: The adhesion of solid particles to flat interfaces and bubbles. Chem. Eng. Sci., 12(2): 133-141.

Omelka, B., Schreithofer, N., Heiskanen, K. (2010). Effect of hydrophobicity and frother concentration on bubble-particle interactions in turbulent flow. XXV IMPC 2010, 3, 2205-2214.

Omelka, B., Schreithofer, N., Wierink, G., Heiskanen, K. (2009). Particle detachment in flotation. In Proc. Procemin, 257–263.

Parthasarathy, R., Jameson, G., Ahmed, N., 1991. Bubble breakup in stirred vessels: Predicting the Sauter mean diameter. Chemical engineering research & design, 69(A4): 295-301.

Pitois, O., Chateau, X., 2002. Small Particle at a Fluid Interface: Effect of Contact Angle Hysteresis on Force and Work of Detachment. Langmuir, 18(25): 9751-9756.

Plate, H., Ph.D. thesis, unpublished.

Princen, A., 1969. Surface Colloid Science. Wiley, New York, USA.

Ralston, J., Fornasiero, D., Hayes, R., 1999. Bubble–particle attachment and detachment in flotation. Int. J. Miner. Process., 56(1–4): 133-164.

Schimann, H.C., 2004. Force and energy measurement of bubble-particle detachment, Master thesis, Virginia Polytechnic Institute and State University.

Schubert, H., 1999. On the turbulence-controlled microprocesses in flotation machines. Int. J. Miner. Process., 56(1-4): 257-276.

Schubert, H., Bischofberger, C., 1978. On the hydrodynamics of flotation machines. Int. J. Miner. Process., 5(2): 131-142.

Schulze, H.J., 1977. New theoretical and experimental investigations on stability of bubble/particle aggregates in flotation: A theory on the upper particle size of floatability. Int. J. Miner. Process., 4(3): 241-259.

Schulze, H.J., 1982. Dimensionless number and approximate calculation of the upper particle size of floatability in flotation machines. Int. J. Miner. Process., 9(4): 321-328.

Schulze, H.J., 1993. Flotation as heterocoagulation process: possibilities of calculating the probability of flotation. Dekker, New York, USA.

Schulze, H.J., Wahl, B., Gottschalk, G., 1989. Determination of adhesive strength of particles within the liquid/gas interface in flotation by means of a centrifuge method. J. Colloid Interface Sci., 128(1): 57-65.

Sherrell, I.M., 2004. Development of a Flotation Rate Equation from First Principles under Turbulent Flow Conditions. Ph.D. thesis, Vierginia Polytechnic Institute and State University.

Shy, S.S., Tang, C.Y., Fann, S.Y., 1997. A nearly isotropic turbulence generated by a pair of vibrating grids. Exp. Therm Fluid Sci., 14(3): 251-262.

Srdic, A., Fernando, H., Montenegro, L., 1996. Generation of nearly isotropic turbulence using two oscillating grids. Exp. Fluids, 20(5): 395-397.

Stevenson, P., Ata, S., Evans, G.M., 2009. The behavior of an oscillating particle attached to a gas-liquid surface. Ind. Eng. Chem. Res., 48(17): 8024-8029.

Sutherland, K., 1948. Physical chemistry of flotation. XI. Kinetics of the flotation process. J. Phys. Chem., 52(2), 394-425.

Tao, D., 2005. Role of bubble size in flotation of coarse and fine particles—A review. Sep. Sci. Technol., 39(4): 741-760.

Taran, E., Nguyen, A.V., 2012. Surface deformation during bubble-particle colloidal interaction quantified by atomic force microscopy and numerical modeling. International Symposium on Separation Technologies for Minerals, Coal, and Earth Resources, Part of the 2011 SME Annual Meeting, Denver, CO, 19-26.

Trahar, W.J., 1981. A rational interpretation of the role of particle size in flotation. Int. J. Miner. Process., 8(4): 289-327.

Van Deventer, J., Feng, D., Burger, A., 2004. Transport phenomena at the pulp–froth interface in a flotation column: II. Detachment. Int. J. Miner. Process., 74(1): 217-231.

Wang, G., Zhou, S., Joshi, J.B., Jameson, G.J., Evans, G.M., 2014. An energy model on particle detachment in the turbulent field. Miner. Eng., 69(0): 165-169.

Wang, G., Evans, G.M., Jameson, G.J., 2016. Bubble–particle detachment in a turbulent vortex I: Experimental. Miner. Eng. 92, 196-207.

Wang, G., Feng, D., Nguyen, A., Evans, G.M., 2016. The dynamic contact angle of a bubble with an immersed-in-water particle and its implications for bubble–particle detachment. Int. J. Miner. Process. 151, 22-32.

Werner, S.c., Hans Joachim, S., 2005. Flotation as a Heterocoagulation Process, Coagulation and Flocculation, Second Edition. Surfactant Science. CRC Press, 455-518.

Welsby, S.D.D., Vianna, S.M.S.M., Franzidis, J.P., 2010. Assigning physical significance to floatability components. Int. J. Miner. Process., 97(1-4): 59-67.

Woodburn, E.T., King, R.P., Colborn, R.P., 1971. The effect of particle size distribution on the performance of a phosphate flotation process. Metallurgical and Materials Transactions B, 2(11): 3163-3174.

Xu, D., Ametov, I., Grano, S.R., 2011. Detachment of coarse particles from oscillating bubbles—The effect of particle contact angle, shape and medium viscosity. Int. J. Miner. Process., 101(1–4): 50-57.

Yoon, R.-H., Mao, L., 1996. Application of Extended DLVO Theory, IV: Derivation of flotation rate equation from first principles. J. Colloid Interface Sci., 181(2): 613-626.

Yoon, R.H., 2000. The role of hydrodynamic and surface forces in bubble–particle interaction. Int. J. Miner. Process., 58(1–4): 129-143.

Young, T., 1805. An essay on the cohesion of fluids. Philos. Trans. R. Soc. Lond., 95: 65-87.

Zhang, M., Wang, G., Evans, G.M., 2016. Flow visualizations around a bubble detaching from a particle in turbulent flows. Miner. Eng. 92, 176-188.

Nomenclature

A	Magnitude of vibration	(m)
A_s	Empirical constant	(-)
Bo	Bond number	(-)
B_o^*	Modified Bond number	(-)
C	Correction to the estimation of the particle detachment energy, Eq.61	(-)
C_p	Particle concentration in the pulp	(kg/m^3)
E_1	Energy barrier	(J)
$E_k^{'}$	Detachment energy	(J)
ΔE_{de}	Particle energy of detachment	(J)
F_a	Centrifugal force	(N)
F_{att}	Attaching force	(N)
F_c	Capillary force	(N)
F_b	Buoyancy force	(N)
F_{de}	Detaching force	(N)
F_g	Gravity force	(N)
F_p	Pressure force	(N)

H	Distance between the bubble apex and the plane of the three phase contact circle	(m)
P_a	Attachment probability	(-)
P_c	Collision probability	(-)
$P_{collection}$	Collection probability	(-)
P_d	Detachment probability	(-)
R_{imp}	Radius of impeller	(m)
R_p	Particle radius	(m)
S	Strength of bubble-particle aggregate	(N)
U_D	Impeller tip velocity	(m/s)
V_g	Gas superficial velocity	(m/s)
ΔV	Turbulent relative velocity between the particle and the bubble	(m/s)
W_a	Work of adhesion	(J)
b_m	Eddy turbulent acceleration	(m/s^2)
$b_{\max}$	Sum acceleration due to circulation and vibration	(m/s^2)
c_1	Constant in fluctuating velocity equation, Eq. 21	(-)
c_2	Particle rotational radius correction factor	(-)
d_{ag}	Diameter of bubble-particle aggregate	(m)

d	Characteristic length scale of particle	(m)
d_B	Bubble diameter	(m)
d_P	Particle diameter	(m)
$d_{b\max}$	Maximum stable bubble diameter	(m)
d_{pmax}	Maximum floatable particle diameter	(m)
$d_{p\min}$	Minimum particle diameter below which detachment probability is zero	(m)
g	Gravity acceleration	(m/s^2)
k	Flotation rate constant	(-)
l	Particle rotating distance from the axis of an eddy	(m)
m_p	Particle mass	(kg)
m_b	Bubble mass	(kg)
r	Radius of rotation	(m)
r_s	Radius of particle movement on bubble surface due to bubble vibration	(m)
p_1	Pressure acting on the particle at the bottom	(pa)
$\overline{u_l}$	Fluctuating velocity corresponding to eddy of scale l	(m/s)
u'	Fluctuating velocity corresponding to eddy of κ-space	(m/s)
u_{ps}	Circular velocity of the attached particle on the vibrating bubble	(m/s)

Greek letters

ω	Rotational speed	(rad/s)
σ	Surface tension	(N/m)
θ_A	Advancing contact angle	(^{o})
θ_R	Receding contact angle	(^{o})
α	Central angle	(^{o})
θ	Contact angle	(^{o})
ρ	Particle density	(kg/m^3)
ρ_l	Liquid density	(kg/m^3)
ρ_P	Particle density	(kg/m^3)
ε	Energy dissipation rate	(m^2/s^3)
κ	Wavenumber of oscillating eddy	(1/m)
α_R	Maximum central angle at attaching process	(^{o})
α_m	Central angle at maximum capillary force	(^{o})
ν	Kinetic viscosity	(m^2/s)
$\varnothing$	Area of contact between particle and bubble	(m^2)
$\Delta\rho$	Density difference between particle and liquid	(kg/m^3)

List of Figures

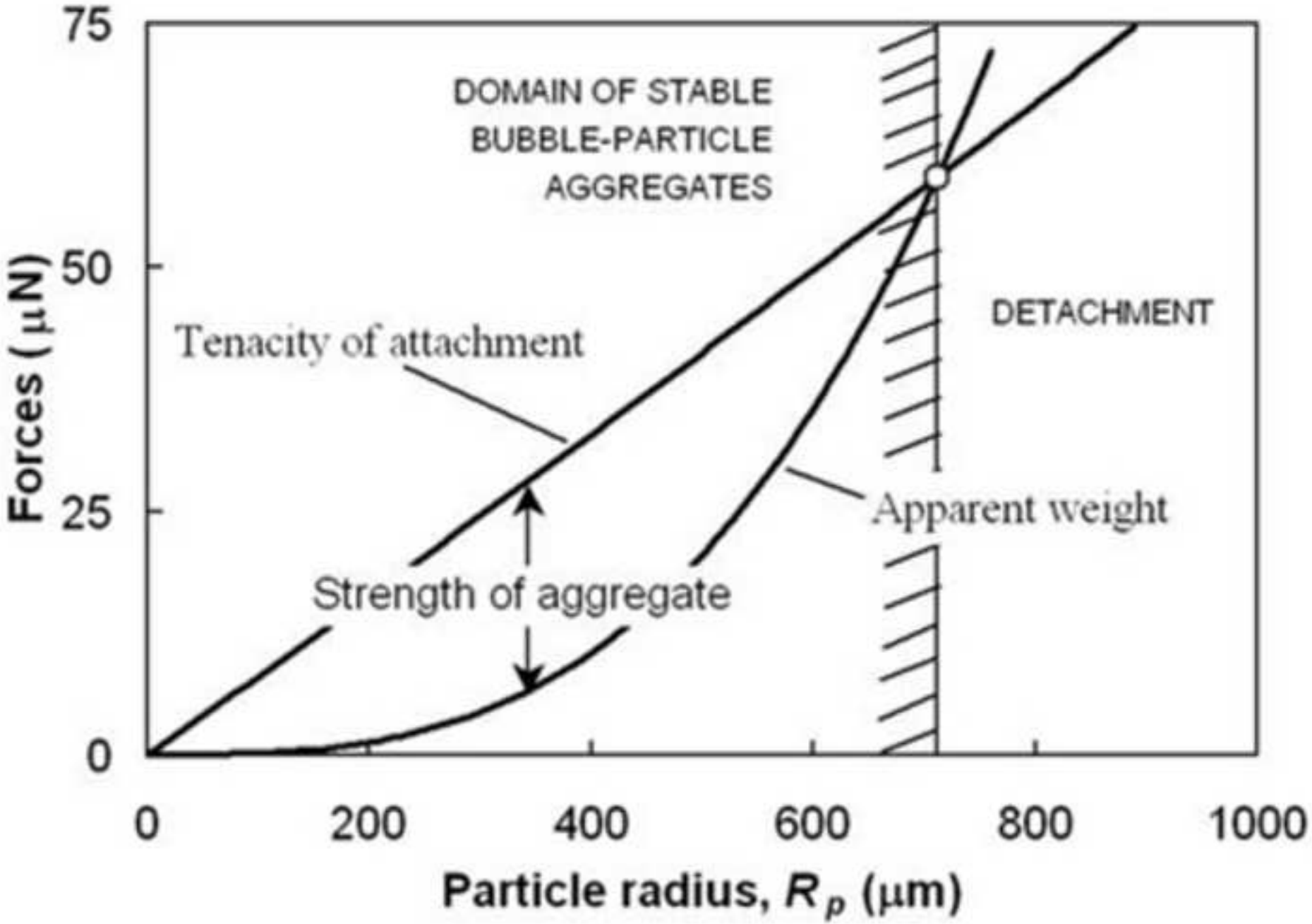

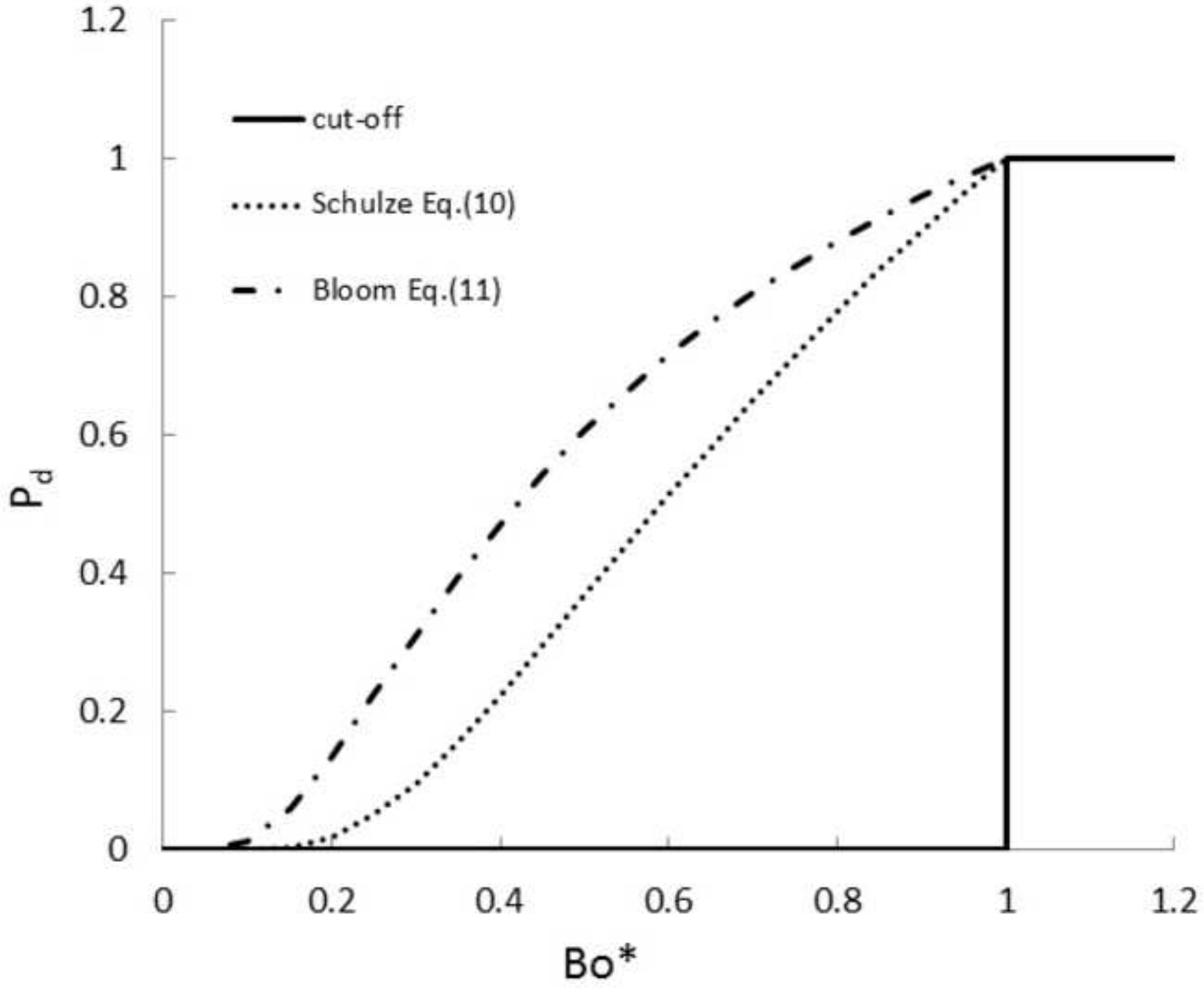

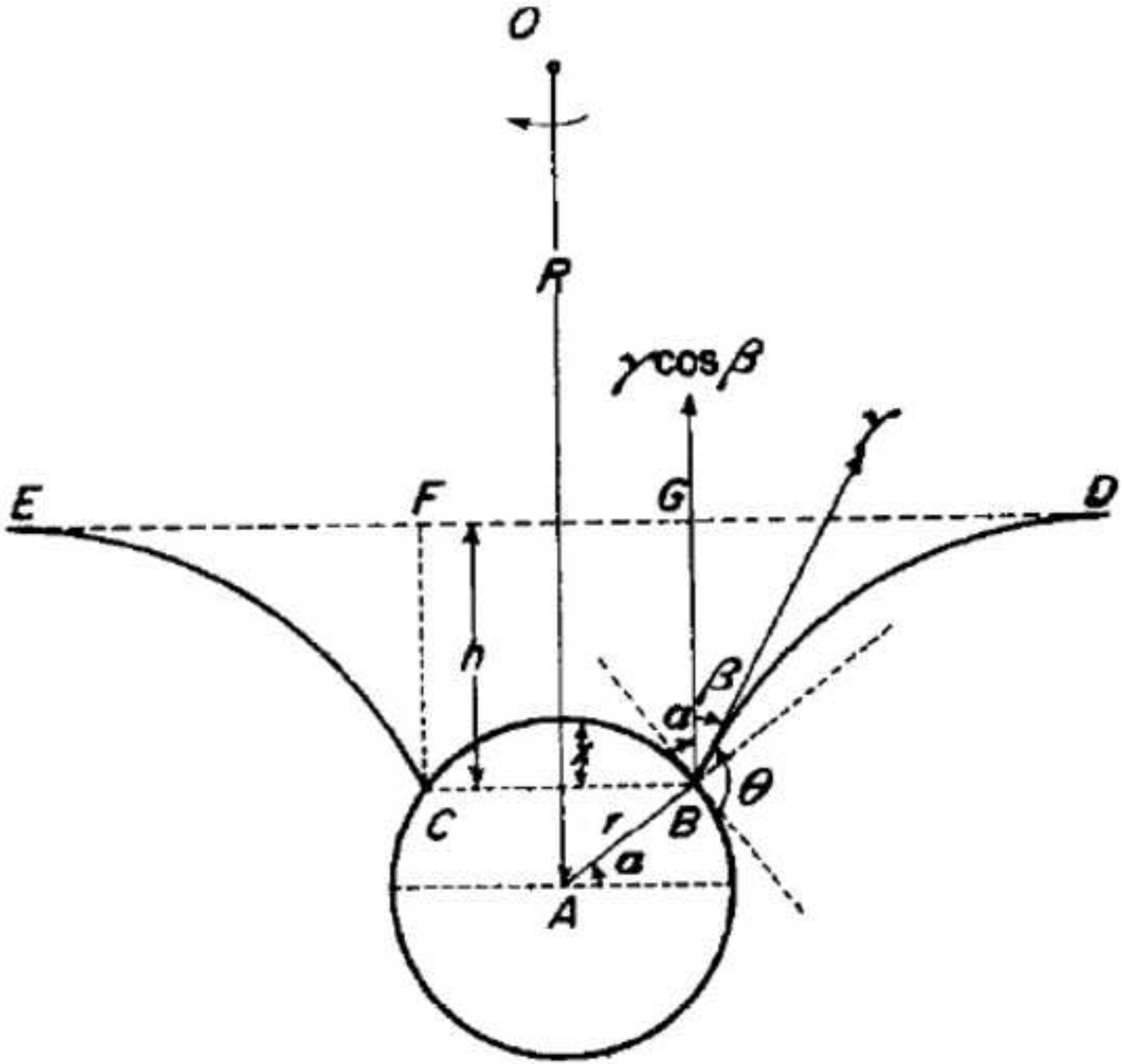

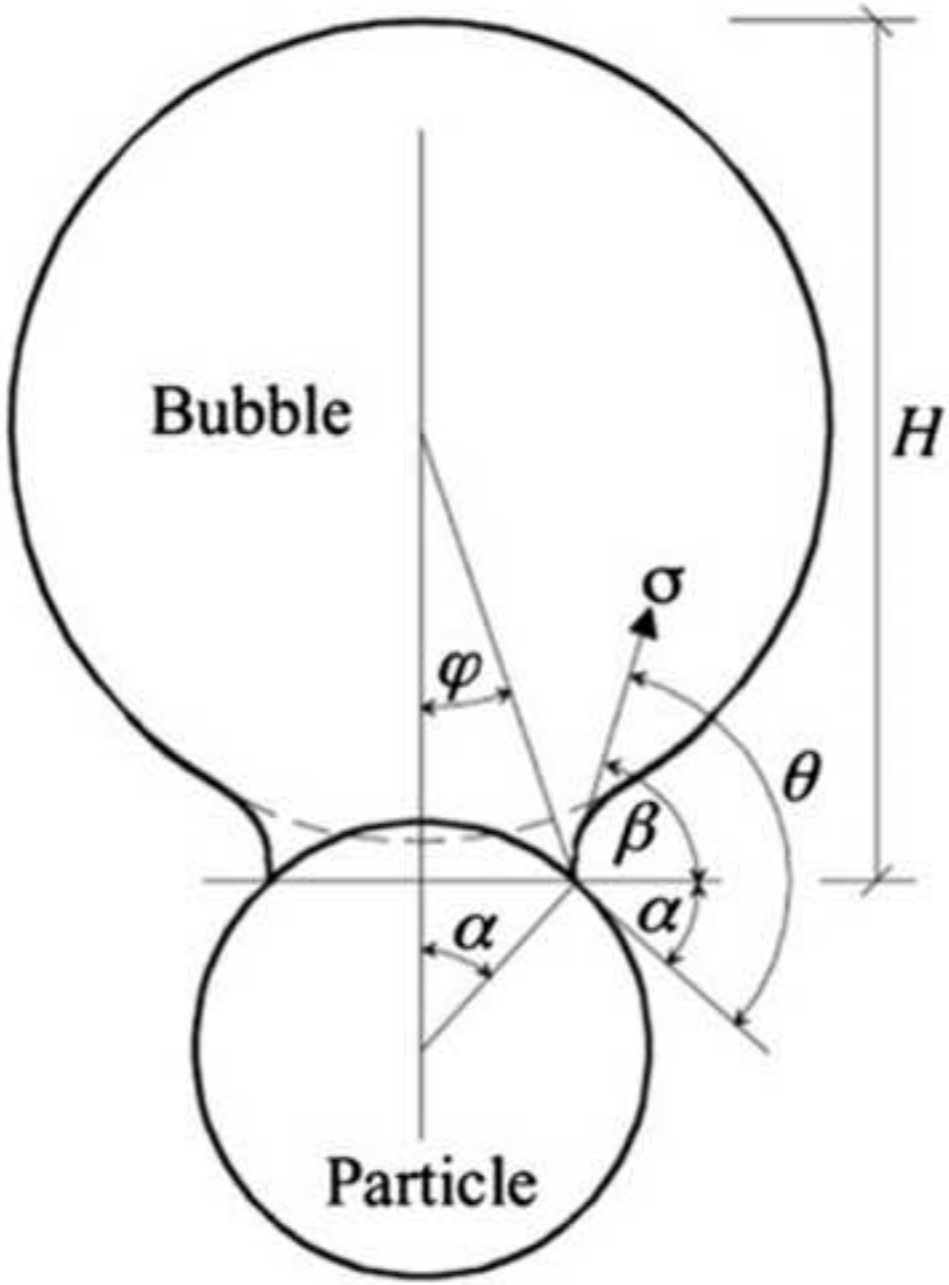

Figures

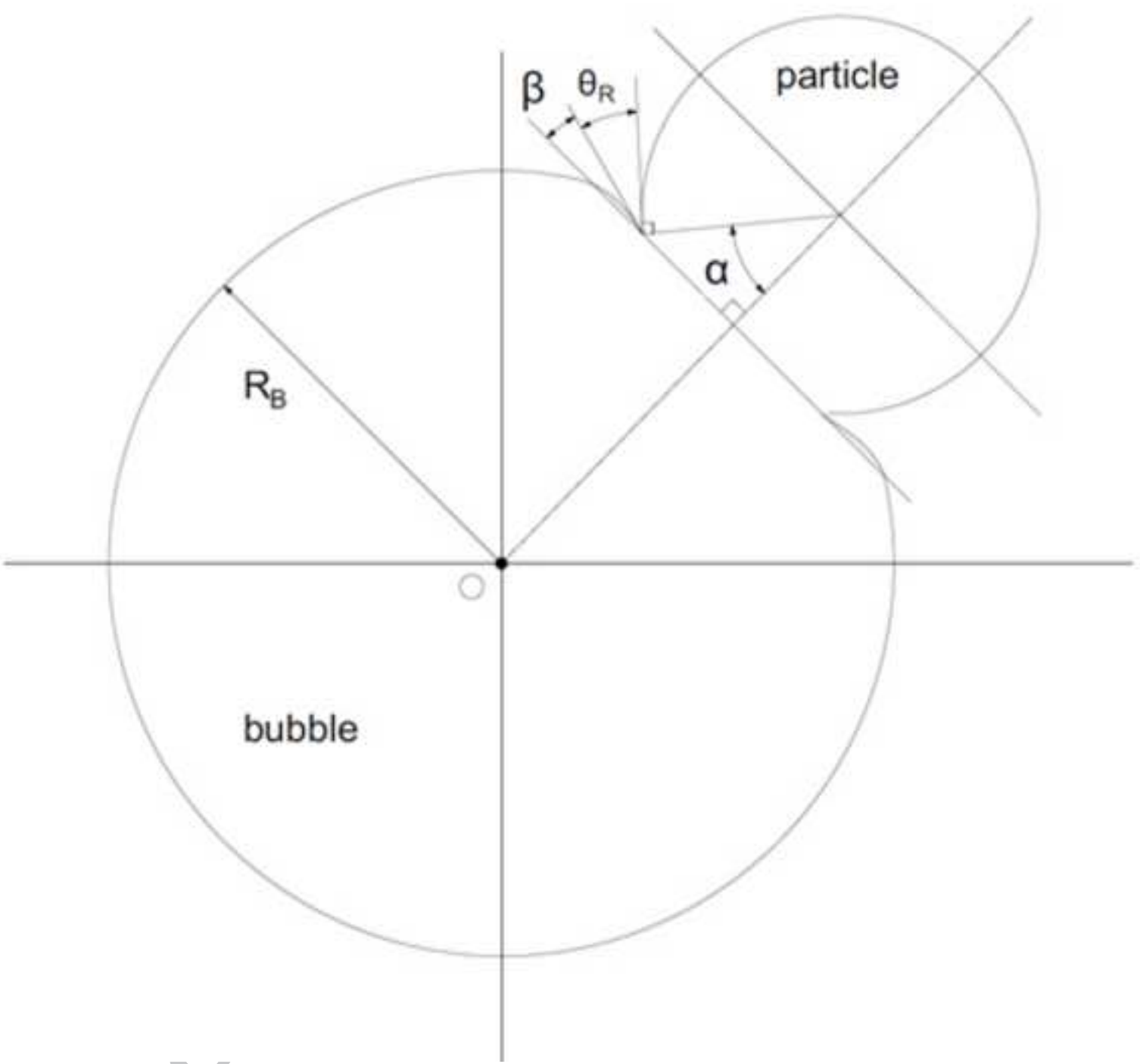

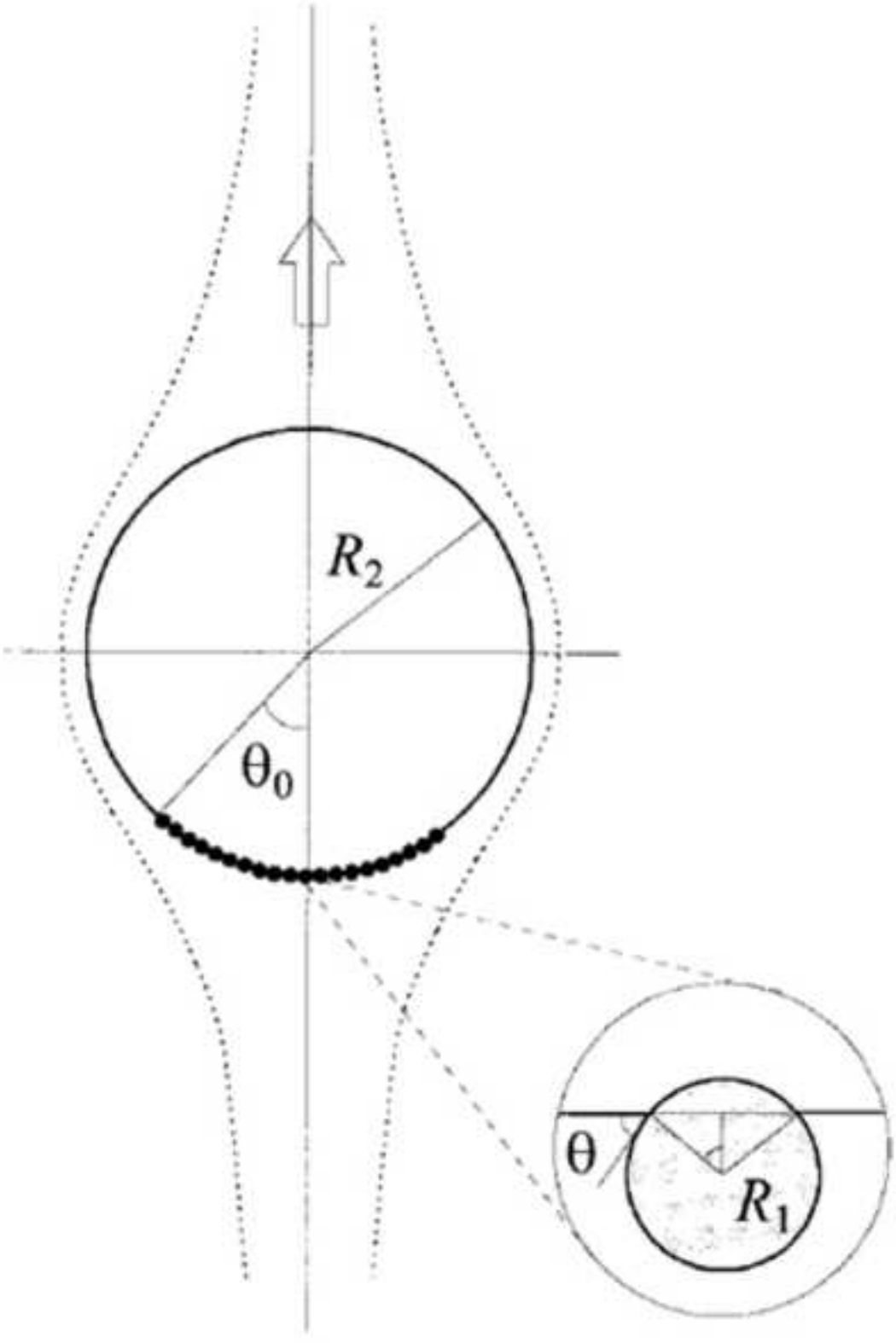

Figures

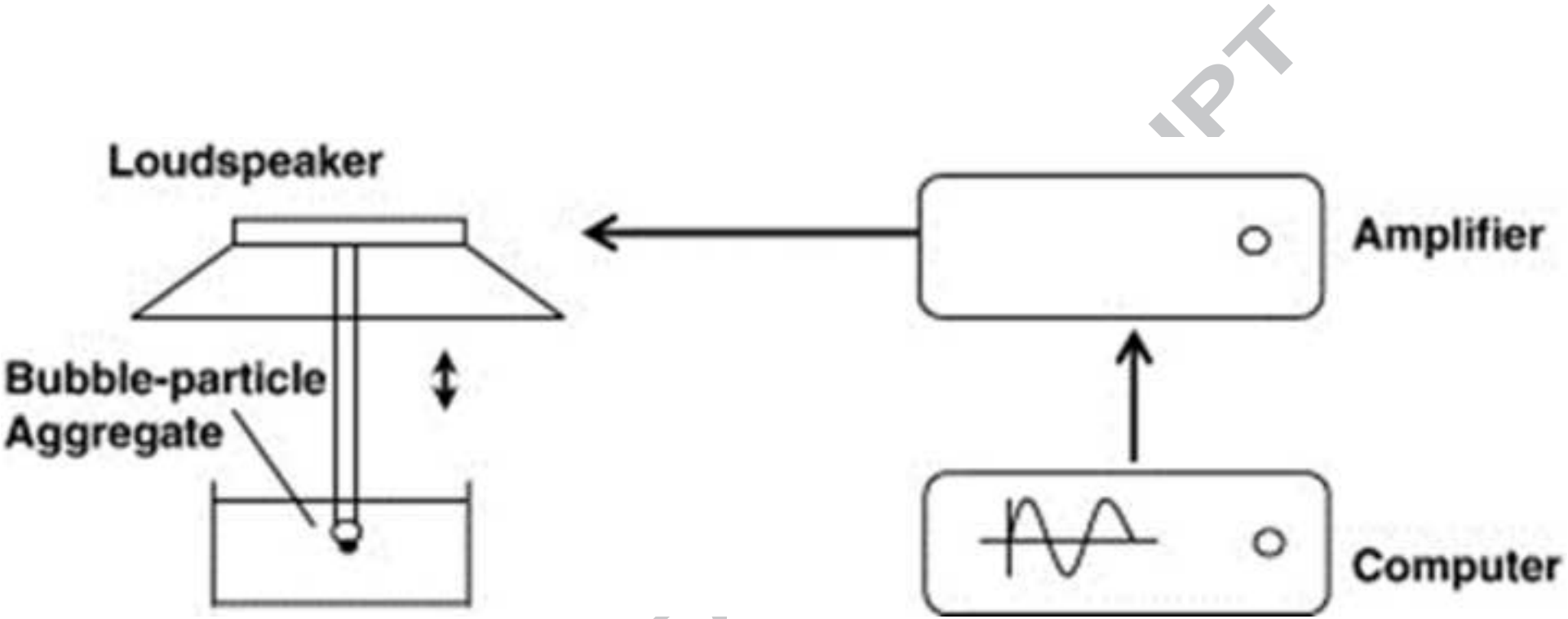

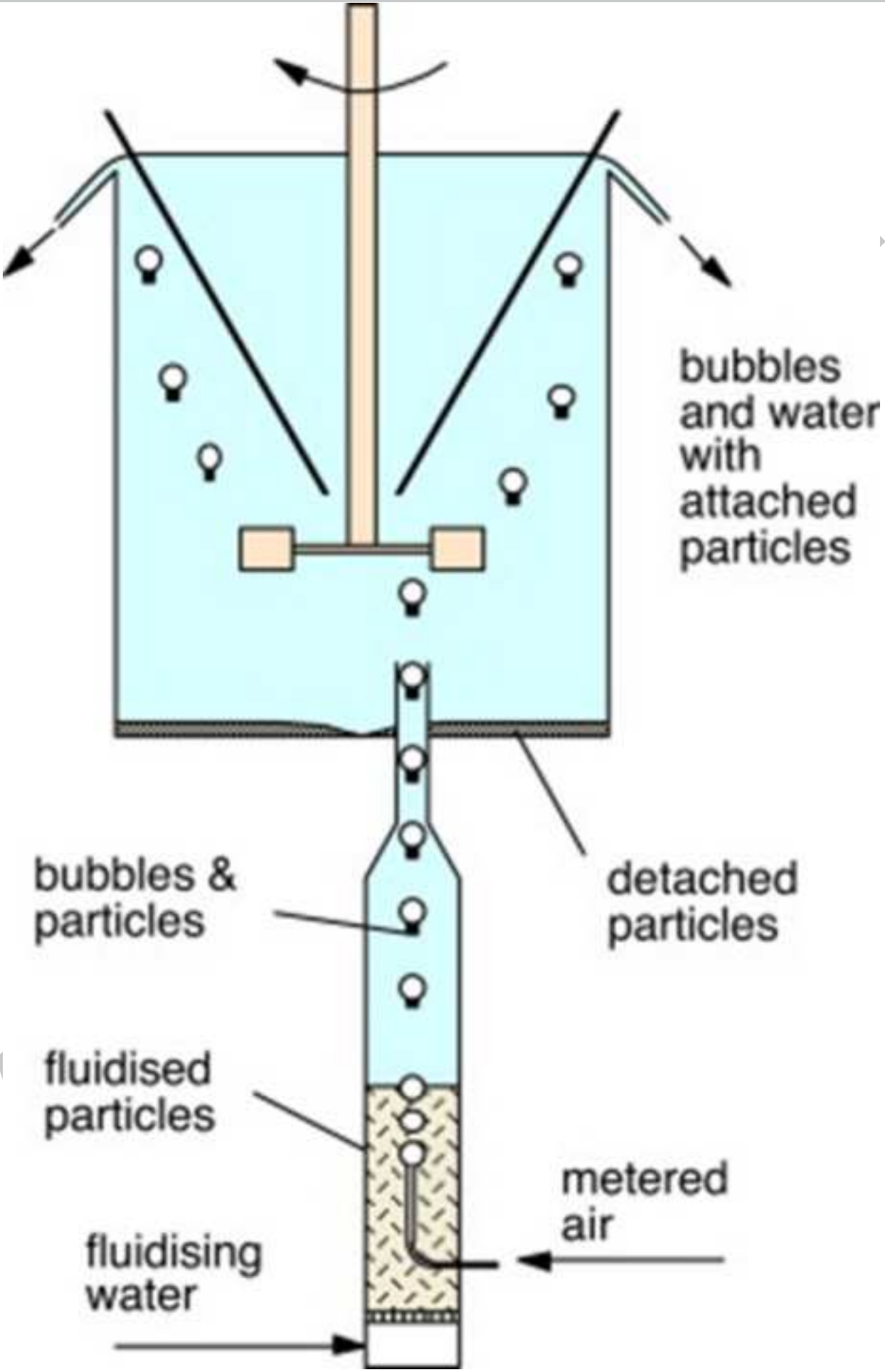

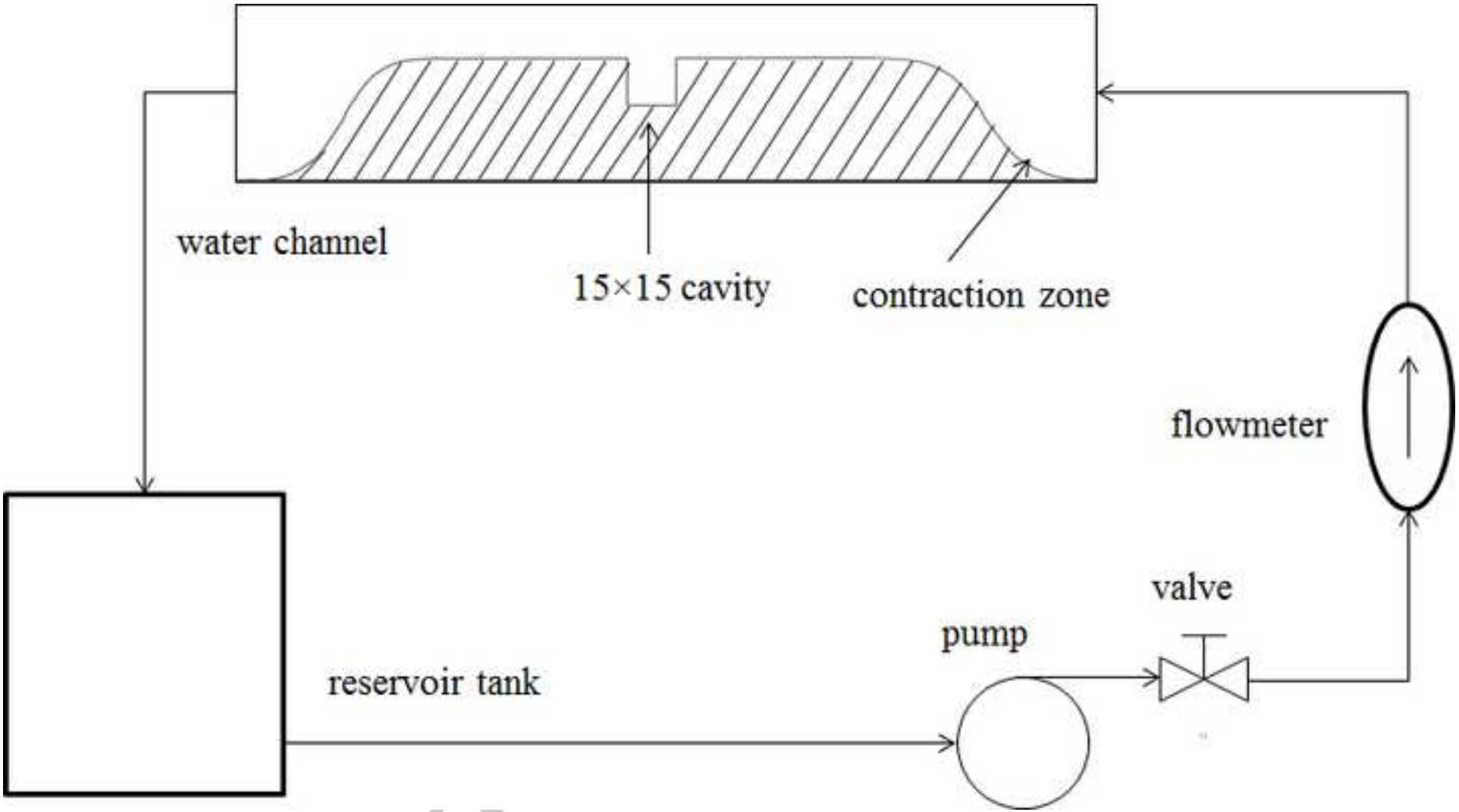

Figures

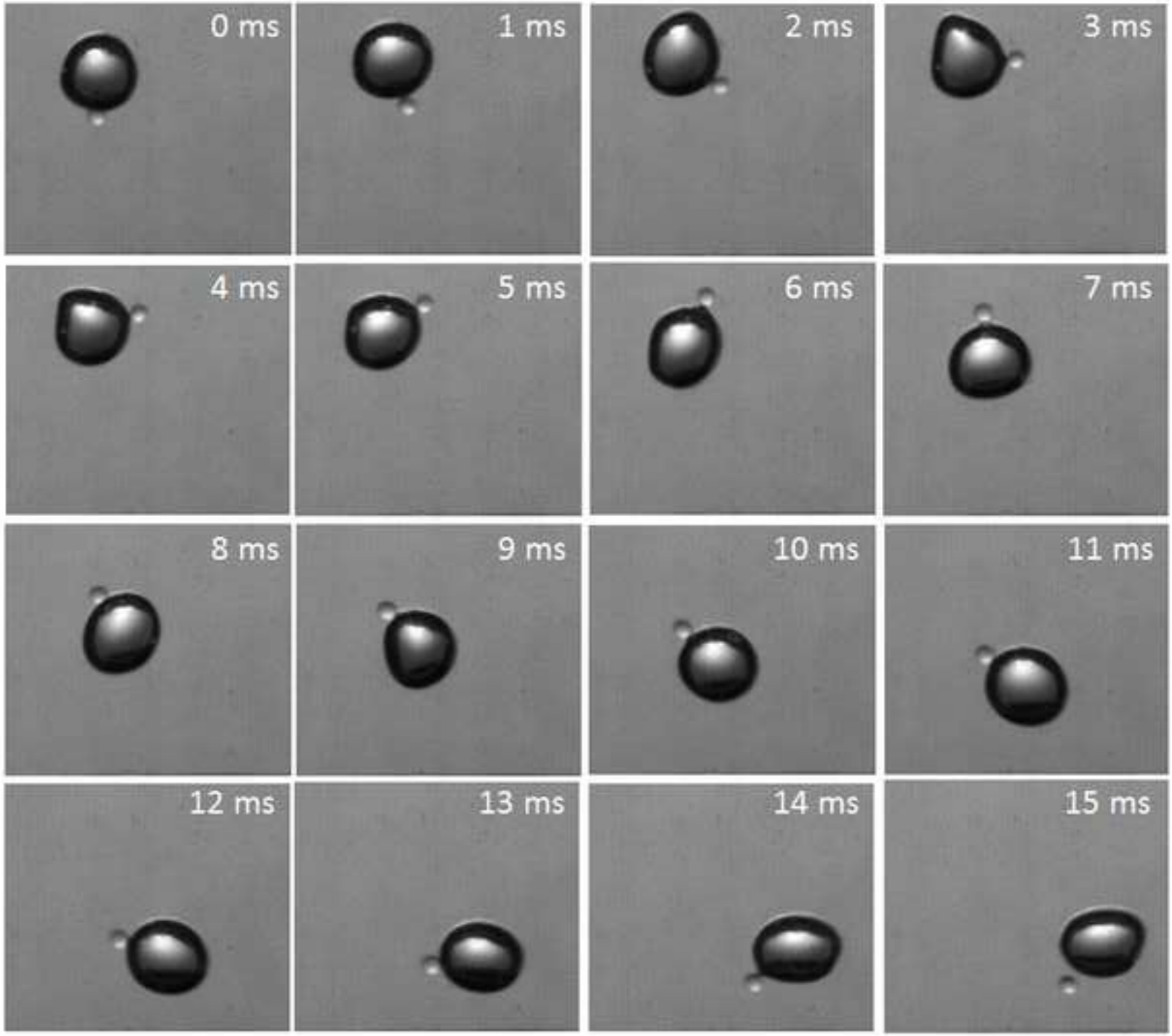

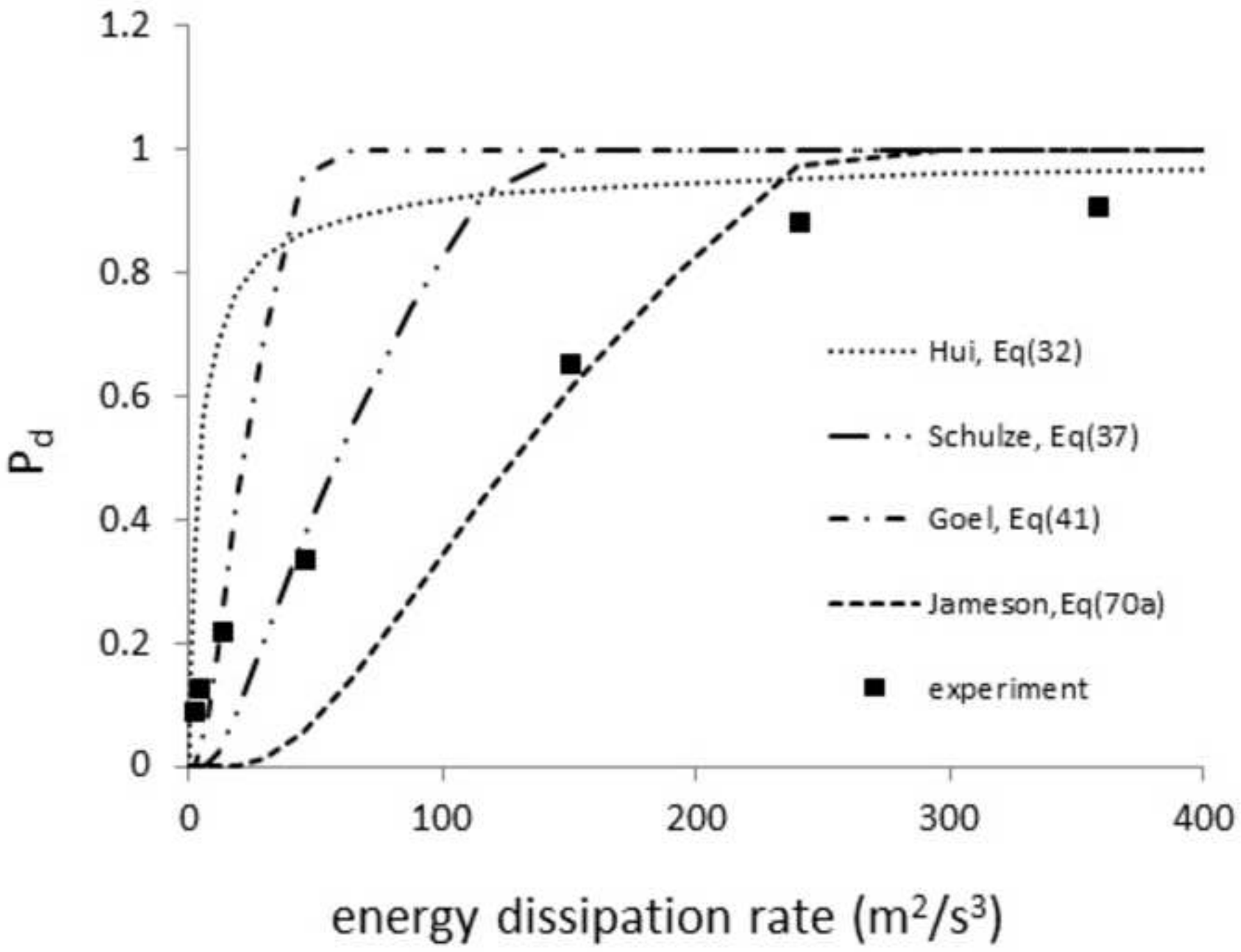

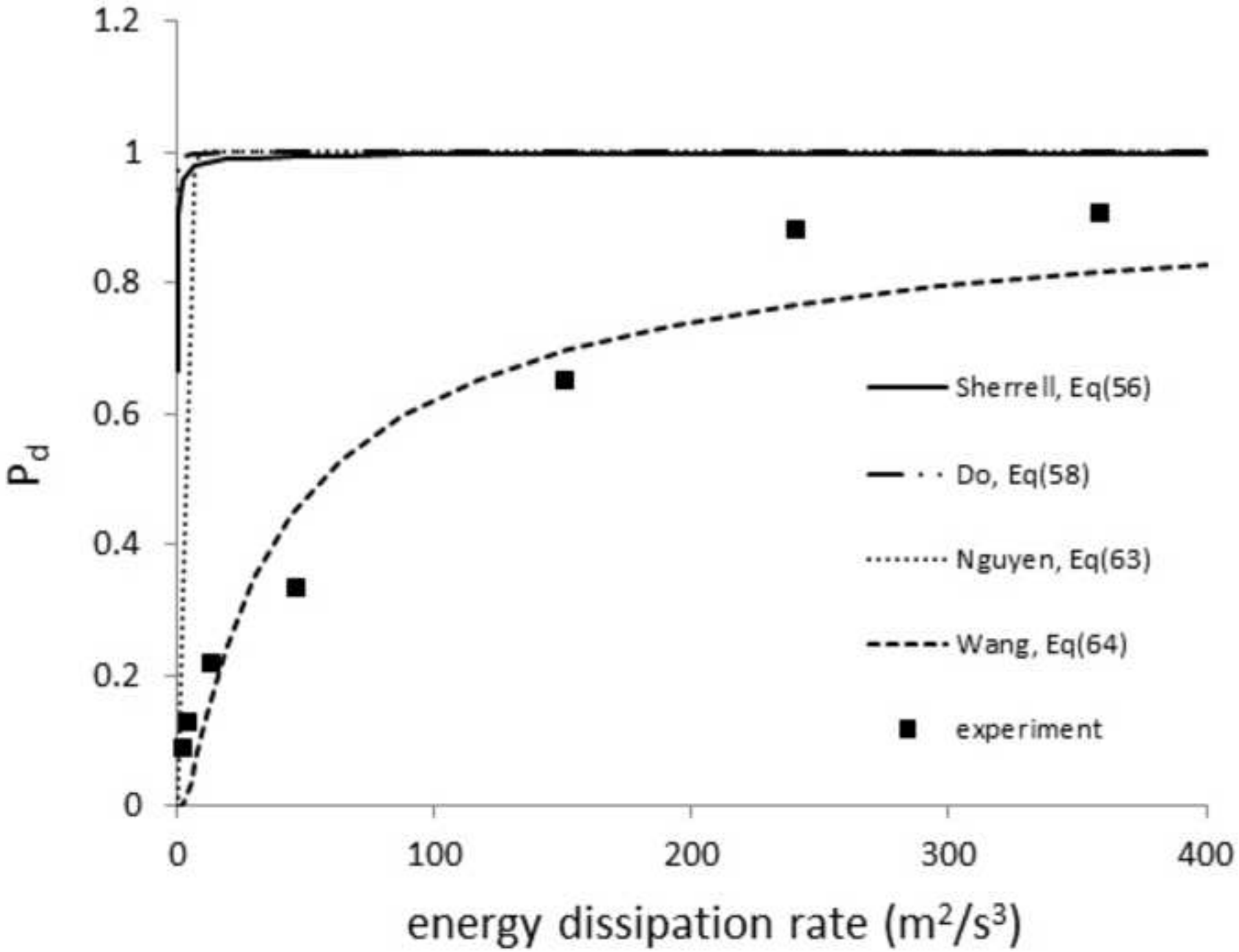

List of tables

Table 1: Summary of detachment models based on force balance

Model	Equation	Comments
Schulze (1993)	$P_d = exp\left\{1-\frac{6\sigma\sin^2\left(\frac{\theta}{2}\right)}{d_P^2\left(g\Delta\rho+\rho_P b_m\right)-d_P\sigma\cos^2\left(\frac{\theta}{2}\right)}\right\}$	Particle rotation
Hui (2001)	$P_d = exp\left(-\frac{\sigma\left(1-\cos\theta\right)d_B^{1/3}}{14.8d_P^2\Delta\rho\varepsilon^{2/3}}\right)$	Bubble oscillation
Nguyen and Schulze (2004)	$P_d = exp\left(1-\frac{3\sigma\left(1-\cos\theta_A\right)}{4R_P^2\left(g+b_m\right)\Delta\rho}\right), \Delta\theta \le \theta_R$ $P_d = exp\left(1-\frac{3\sigma\sin\theta_R\sin\left(\Delta\theta\right)}{4R_P^2\left(g+b_m\right)\Delta\rho}\right), \Delta\theta \ge \theta_R$	Particle rotation
Nguyen and Schulze (2004)	$P_d = exp\left(1-\frac{\sigma\left(1-\cos\theta_A\right)\sin\left(\Delta\theta/2\right)}{0.26\pi R_P\rho_l\sqrt{\varepsilon\nu}}\right), \Delta\theta \le \theta_R$ $P_d = exp\left(1-\frac{\sigma\sin\theta_R\sin(\Delta\theta)\sin\left(\Delta\theta/2\right)}{0.13\pi R_P\rho_l\sqrt{\varepsilon\nu}}\right), \Delta\theta \ge \theta_R$	Shear force
Tao (2005)	$P_d = \frac{1}{1+\frac{3\sigma\left(1-\cos\theta_d\right)}{g\left(\rho_P-\rho_l\pi\left(1/2+3/4\times\cos\left(\theta_d/2\right)\right)\right)}\frac{1+d_P/d_B}{d_P^2}}$	Steady case
Goel and Jameson (2012)	$P_d = exp\left(1-\frac{6\sigma\sin^2\left(\frac{\theta}{2}\right)}{3.75d_P^2\rho_P\varepsilon^{2/3}/d_B^{1/3}}\right)$	Particle rotation

Table 2: Summary of detachment models based on energy balance

Model	Equation	Comments
Yoon and Mao (1996)	$P_d = exp\left(-\frac{\sigma\pi R_p^2 \left(1-\cos\theta\right)^2 + E_1}{\frac{\rho g R_B^2 \theta_0}{3} \pi R_P^2 \sin^2\theta} \right)$	Steady case.
Sherrell (2004)	$P_d = exp\left(-\frac{\sigma\pi R_p^2 \left(1-\cos\theta\right)^2}{\frac{1}{2}\left(m_p + m_b\right)\left(R_{imp}\omega\right)^2} \right)$	Limited to stirred tank
Nguyen and Schulze (2004)	$P_d = exp\left(1-\frac{3\sigma\left(1-\cos\theta\right)^2 \times C}{2R_P \Delta\rho \left(\Delta V\right)^2} \right)$ $C = \frac{1}{4}\ln\frac{2L/R_P/\sin\left(\theta/2\right)}{e^{\gamma}\cos^2\left(\theta/4\right)} + \frac{13+16\cos\left(\theta/2\right)+7\cos\theta}{64\cos^4\left(\theta/4\right)}$	General shear flow
Do (2010)	$P_d = exp\left(-\frac{\sigma\pi R_p^2 \left(1-\cos\theta\right)^2}{\frac{1}{2} m_p \left(\left(d_P + d_B\right)\sqrt{\varepsilon/\nu}\right)^2} \right)$	General shear flow
Wang et al. (2014)	$P_d = \exp\left(-\frac{8\sigma R_p^2 \left(1-\cos\theta\right)^2}{c\rho_l \varepsilon^{2/3} d_p^{11/3}} \right)$	Isotropic turbulence

Table 3: Summary of detachment models based on maximum floatable particle size

Model	Equation	Comments
Woodburn et al. (1971)	$P_d = \left(\frac{d_p}{d_{pmax}} \right)^{1.5}$, $\mathrm{d_p} \le \mathrm{d_{pmax}}$ $P_d = 1, \mathrm{d_p} > \mathrm{d_{pmax}}$	Maximum floatable particle is required
Jameson et al. (2007)	$P_d = exp\left(1 - \frac{2.34\sigma^{6/5}(1-\cos\theta)}{d_p^2 \Delta\rho\varepsilon^{4/5}\rho_l^{1/5}} \right), \Delta\theta \le \theta_R$ $P_d = exp\left(1 - \frac{1.17\sigma^{6/5}\sin\theta_R \sin\Delta\theta}{d_p^2 \Delta\rho\varepsilon^{4/5}\rho_l^{1/5}} \right), \Delta\theta \ge \theta_R$	Energy dissipation rate is required
Brożek and Młynarczykowska (2010)	$P_d = \left(\frac{d_p - d_{p\min}}{d_{p\max} - d_{p\min}} \right)^n$	Maximum floatable particle is required

Highlights

1. Bubble-particle detachment models in flotation are reviewed.
2. Experimental works highlighting the detachment mechanisms are reviewed.
3. Detachment probabilities predicted from detachment models are compared.